Supporting information

Cationic indium complexes for the copolymerization of functionalized epoxides with cyclic ethers and lactide

*Carlos Diaz, Tannaz Ebrahimi and Parisa Mehrkhodavandi**

University of British Columbia, Department of Chemistry, 2036 Main Mall, Vancouver, BC, Canada, V6T 1Z1.

Parisa Mehrkhodavandi (mehr@chem.ubc.ca).

Contents

A. Experimental section

General Considerations. Unless otherwise indicated, all air- and/or water-sensitive reactions were carried out under dry nitrogen using either an MBraun glove box or standard Schlenk line techniques. NMR spectra were recorded on a Bruker Avance 300 MHz, 400 MHz and 600 MHz spectrometer. ^{1}H NMR chemical shifts are reported in ppm versus residual protons in deuterated solvents as follows: δ 7.27 $CDCl_3$, $^{13}C\{^{1}H\}$ NMR chemical shifts are reported in ppm versus residual ^{13}C in the solvent: δ 77.2 $CDCl_3$. $^{19}F\{^{1}H\}$ NMR chemical shifts are reported in ppm and externally referenced to neat $CFCl_3$ at 0 ppm. For kinetic and conversion measurements TMB (1,3,5-trimethoxybenzene) was used as an internal standard. Diffraction measurements for X-ray crystallography were made on a Bruker X8 APEX II diffraction and a Bruker APEX DUO diffraction with graphite monochromated Mo-Kα radiation. The structures (Appendix C) were solved by direct methods and refined by full-matrix least-squares using the SHELXTL crystallographic software of Bruker-AXS. Unless specified, all non-hydrogens were refined with anisotropic displacement parameters, and all hydrogen atoms were constrained to geometrically calculated positions but were not refined. EA CHN analysis was performed using a Carlo Erba EA1108 elemental analyzer. The elemental composition of unknown samples was determined by using a calibration factor. The calibration factor was determined by analyzing a suitable certified organic standard (OAS) of a known elemental composition. Molecular weights were determined by triple detection gel permeation chromatography (GPC-LLS) using a Waters liquid chromatograph equipped with a Water 515 HPLC pump, Waters 717 plus autosampler, Waters Styragel columns (4.6 × 300 mm) HR5E, HR4 and HR2, Water 2410 differential refractometer, Wyatt tristar miniDAWN (laser light scattering detector) and a Wyatt ViscoStar viscometer. A flow rate of 0.5 mL min^{-1} was used and samples were dissolved in THF (2 mg mL^{-1}). Narrow molecular weight polystyrene standards were used for calibration purposes. The dn/dc (differential refractive index increment) values of the polymers studied were determined by running external calibration curves or by calculation of the GPC software assuming >90% mass recovery.

Materials. Solvents (THF, 2-Methyl THF, tetrahydropyran and hexanes) were dried and vacuum-distilled over sodium, using benzophenone as an indicator and degassed through a series of freeze-pump-thaw cycles. Toluene was dried and distilled over CaH_2. Deuterated solvents ($CDCl_3$, d^8-Tol, C_6D_5Br and CD_3CN) were dried over CaH_2, collected by vacuum distillation and also degassed. Benzyl potassium was synthesized by the reaction of n-buthyl lithium with potassium tert-butoxide in cold toluene and isolated as a red solid that was washed with hexanes and dried under vacuum. Indium trichloride ($InCl_3$) was purchased from Tokyo Chemical Industries (TCI) and used as received. Silver hexaflurophosphate ($AgPF_6$), silver hexafluroarsenate ($AgAsF_6$), silver hexafluoroantimonate ($AgSbF_6$) and silver tetrafluoroborate ($AgBF_4$) were purchased from Alfa Aesar and used as received. Epoxide monomers were dried over CaH_2, distilled and stored under molecular sieves. *Rac*-lactide was recrystallized 3 times from dry toluene and dried under vacuum. (±)-(ONNO)InCl was prepared according to published methodologies.[1]

Synthesis of (±)-[(ONNO)In(THF)$_2$][SbF$_6$] (3). A 20 mL scintillation vial was charged with a stirbar, (±)-(ONNO)InCl (0.15 g, 0.22 mmol) and 6 mL of THF, and the resulting solution was cooled down to −30 °C. A suspension of $AgSbF_6$ (0.076 g, 0.22 mmol) in 10 mL of THF was generated, cooled down to −30 °C, and was added to the (±)-(ONNO)InCl solution with constant stirring. The formation of a precipitate was observed immediately after this addition addition. The reaction was left stirring in the dark at room temperature for 20 min. The resulting mixture was filtered through Celite and dried under vacuum to produce a pale yellow solid 91% yield, which was used without further purification. Small crystals suitable for X-ray diffraction could be obtained from a THF/toluene solution. ^{1}H NMR (300 MHz, $CDCl_3$, 25 °C): δ 8.48 (2H, s, N=C*H*), 7.53 (2H, s, Ar*H*), 7.08 (2H, s, Ar*H*), 3.69 (8H, br m, O-CH_2 of THF), 3.47 (2H, m, -C*H*-), 2.68 (2H, m, -CH_2-), 2.06 (2H, m, -CH_2-),

1.82 (8H, br m, -C*H*$_2$- of THF), 1.61 (4H, br m, -C*H*$_2$-), 1.46 (18H, s, -C(C*H*$_3$)$_3$), 1.33 (18H, s, -C(C*H*$_3$)$_3$). ^{13}C{^{1}H} NMR (101 MHz, $CDCl_3$, 25 °C): δ 170.16, 166.89, 141.47, 138.59, 131.21, 117.36, 69.53, 63.95, 35.63, 34.45, 31.35, 29.43, 27.10, 25.32, 23.46. ^{19}F NMR (376 MHz, CD_3CN, 25 °C): δ −110.82, −113.89, −115.97, −119.44, −121.08, −122.24, −125.06, −126.25, −127.84, −131.39, −133.42, −136.51. Anal. Calcd. (found) for $C_{44}H_{68}O_4N_2InSbF_6$ (**3**): C 50.84 (50.82), H 6.65 (6.59), N 2.58 (2.69).

Synthesis of (±)-[(ONNO)In(THF)$_2$][BF$_4$] (4). Complex **4** was generated using a similar procedure to complex **3**, but was obtained in a mixture of decomposition products and could not be purified. Small crystals suitable for X-ray diffraction could be obtained from a THF/toluene solution.

Synthesis of (±)-[(ONNO)In(THF)$_2$][A] (A = PF$_6$ (1), AsF$_6$ (2)): Complexes **1** and **2** were generated using a similar procedure to complex **3**, with an additional steps (due to the lower purity of silver salts): the solid products were suspended in dichloromethane, filtered through Celite and then tetrahydrofuran was added to them. Drying under vacuum afforded pale yellow solids, both in 85% yields. Small crystals of the ACN adduct of **1**, suitable suitable for X-ray diffraction could be obtained from a THF/toluene/ACN solution. ^{1}H and ^{13}C{^{1}H} NMR spectra of both complexes were identical to those of 3. ^{19}F NMR (**1**) (376 MHz, $CDCl_3$, 25 °C): δ −70.12, −70.23. Anal. Calcd. (found) for $C_{44}H_{68}O_4N_2InPF_6$ (**1**): C 55.70 (55.63), H 7.22 (7.02), N 2.95 (2.99). Anal. Calcd. (found) for $C_{44}H_{68}O_4N_2InAsF_6$ (**2**): C 53.23 (53.29), H 6.90 (6.85), N 2.82 (2.88).

Synthesis of (±)-[(ONNO)In(Me-THF)$_2$][SbF$_6$] (5): Synthesized in an analogous manner to **3**, using 2-methyl tetrahydrofuran (Me-THF) as a solvent and was obtained as a pale yellow solid in a 92% yield. ^{1}H NMR (300 MHz, $CDCl_3$, 25 °C): δ 8.46 (2H, s, N=C*H*), 7.54 (2H, s, Ar*H*), 7.08 (2H, s, Ar*H*), 4.22 (2H, br m, O-C*H* of Me-THF), 3.78 (4H, br m, O-C*H*$_2$ of Me-THF), 1.95 (4H, overlapping m, -C*H*$_2$- of Me-THF), 1.47 (18H, s, -C(C*H*$_3$)$_3$), 1.32 (18H, s, -C(C*H*$_3$)$_3$), 1.05 (6H, d, -C*H*$_3$ of Me-THF). ^{13}C{^{1}H} NMR (101 MHz, $CDCl_3$, 25 °C): δ 170.61, 166.90, 141.55, 138.97, 131.29, 131.21, 117.49, 77.56, 68.85, 63.86, 35.59, 34.07, 32.34, 31.28, 29.48, 27.41, 24.94, 23.66, 20.88. Anal. Calcd. (found) for $C_{46}H_{72}O_4N_2InSbF_6$: C 51.75 (51.59), H 6.80 (6.97), N 2.62 (2.53).

Synthesis of (±)-[(ONNO)In(THP)$_2$][SbF$_6$] (6): Synthesized in an analogous manner to **3**, using tetrahydropyran (THP) as a solvent and was obtained as a pale yellow solid in a 85% yield. ^{1}H NMR (300 MHz, $CDCl_3$, 25 °C): δ 8.48 (2H, s, N=C*H*), 7.54 (2H, s, Ar*H*), 7.08 (2H, s, Ar*H*), 3.64 (8H, br m, O-C*H*$_2$ of THP), 1.57 (12H, br overlapping m, -C*H*$_2$- of THP), 1.49 (18H, s, -C(C*H*$_3$)$_3$), 1.32 (18H, s, -C(C*H*$_3$)$_3$). ^{13}C{^{1}H} NMR (101 MHz, $CDCl_3$, 25 °C): δ 170.79, 167.01, 141.77, 139.02, 131.28, 131.11, 117.34, 69.87, 64.03, 35.62, 34.08, 31.27, 29.56, 27.42, 26.17, 23.68, 22.71. Anal. Calcd. (found) for $C_{46}H_{72}O_4N_2InSbF_6$: C 51.75 (52.48), H 6.80 (7.04), N 2.62 (2.52).

Synthesis of (±)-[(ONNO)In(THF)][OTf]: Synthesised in an analogous manner to complex **3**, using THF as the reaction solvent and was obtained as a pale yellow solid in a 90% yield. ^{1}H NMR (300 MHz, $CDCl_3$, 25 °C): δ 8.37 (2H, s, N=C*H*), 7.53 (2H, s, Ar*H*), 6.99 (2H, s, Ar*H*), 3.76 (3H, br m, O-C*H*$_2$ of THF), 2.60 (2H, m, -C*H*-), 2.10 (2H, m, -C*H*$_2$-), 1.84 (3H, br m, -C*H*$_2$- of THF), 1.47 (18H, s, -C(C*H*$_3$)$_3$), 1.31 (18H, s, -C(C*H*$_3$)$_3$).

Representative polymerization of epoxides with complex 3 in solution. A Schlenk flask was charged with a solution of complex **3** (20.2 mg, 0.019 mmol) in 0.6 mL of C_6H_5Br. 1,2-Epoxy-5-hexene (0.44 mL, 3.9 mmol) was added directly to the flask by a syringe. The mixture was stirred at 25 °C for 24 h. The resulting solution was concentrated under vaacuum for 3 h and then cold methanol

was added to it (0 °C, 15 mL). The polymer precipitated from solution and was isolated by decantation or centrifugation. The isolated polymer was dried under high vacuum for at least 3 h prior to analysis.

Representative polymerization of epoxides with complex 3 for NMR monitoring. A J Young NMR tube was charged with a solution of complex **3** (20.2 mg, 0.019 mmol) in 0.5 mL of C_6D_5Br. The solution was frozen with liquid nitrogen and then a solution of 1,3,5-trimethoxybenzene (8.6 mg, 0.051 mmol) in 0.1 mL of C_6D_5Br was subsequently added to it. The solution was frozen with liquid nitrogen and then a solution of 1,2-Epoxy-5-hexene (0.22 mL, 1.9 mmol) in 0.1 mL of C_6D_5Br was added to it and frozen with liquid nitrogen. The J Young tube was put under vaccuum and closed and the mixture in the tube was kept frozen under liquid nitrogen prior to analysis. To study the effect of PF_6 ions on this system, a similar procedure was employed, but with the addition of KPF_6 (3.6 mg, 0.019 mmol) to the 1,3,5-trimethoxybenzene solution in 0.1 mL of C_6D_5Br.

Representative copolymerization of epoxides and other cyclic ethers with complex 3 in solution. A Schlenk flask was charged with a solution of complex **3** (40.3 mg, 0.039 mmol) in 0.6 mL C_6H_5Br and THF (0.31 mL, 3.8 mmol). 1,2-Epoxy-5-hexene (0.44 mL, 3.9 mmol) was added directly to the flask by a syringe. The mixture was stirred at 25 °C for for 4 days. The resulting solution was concentrated under vacuum for 3 h and then cold methanol was added to it (0 °C, 15 mL). The polymer precipitated from solution and was isolated by decantation. The isolated polymer was dried under high vacuum for at least 3 h prior to analysis.

Representative co-polymerization of epoxides and *rac*-lactide with complex (3). In a glovebox, a schlenk flask was charged with complex **3** (13.3 mg, 0.013 mmol) and epichlorohydrin (0.1 mL, 1.3 mmol) was added directly to the flask by a syringe. Then *rac*-lactide was added (343.6 mg, 2.4 mmol) and the flask was sealed and heated to 130 °C for for 1 h. The reaction was then cooled to room temperature and the solid residue was suspended in a small amount of dichloromethane, after which cold methanol was added to it (0 °C, 15 mL). The polymer precipitated from solution and was isolated by decantation or centrifugation. The isolated polymer was dried under high vacuum for at least 3 h prior to analysis.

B. Characterization of complexes in solution

(S1a)

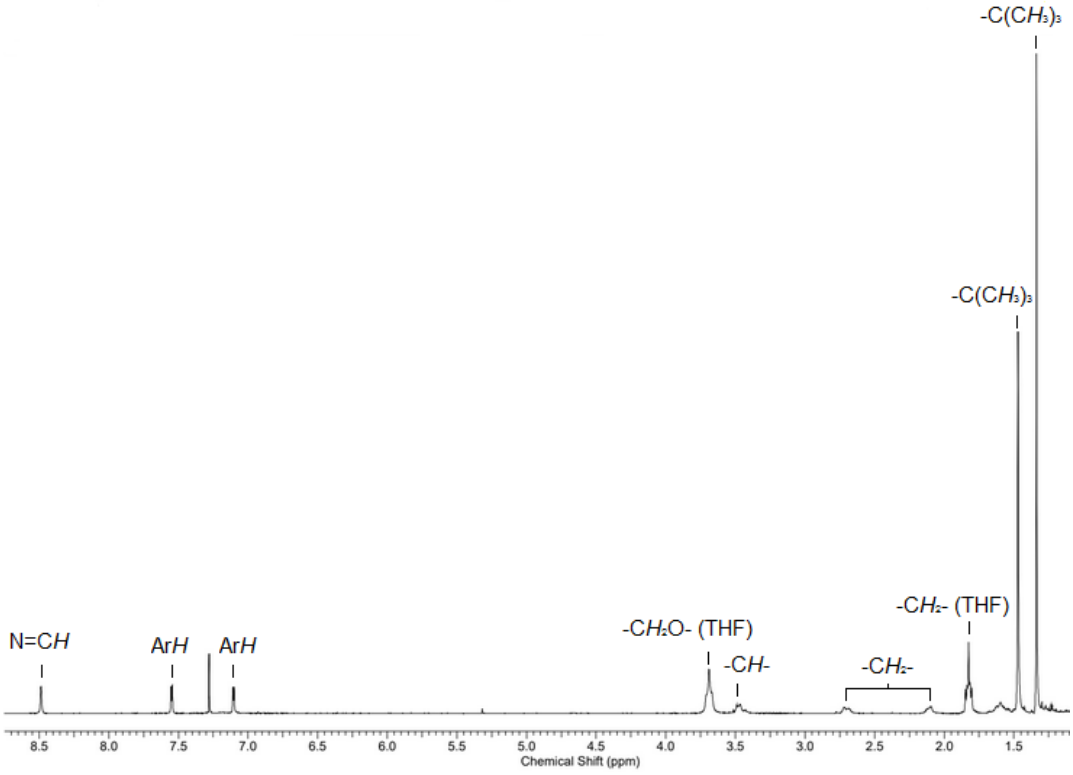

(S1b)

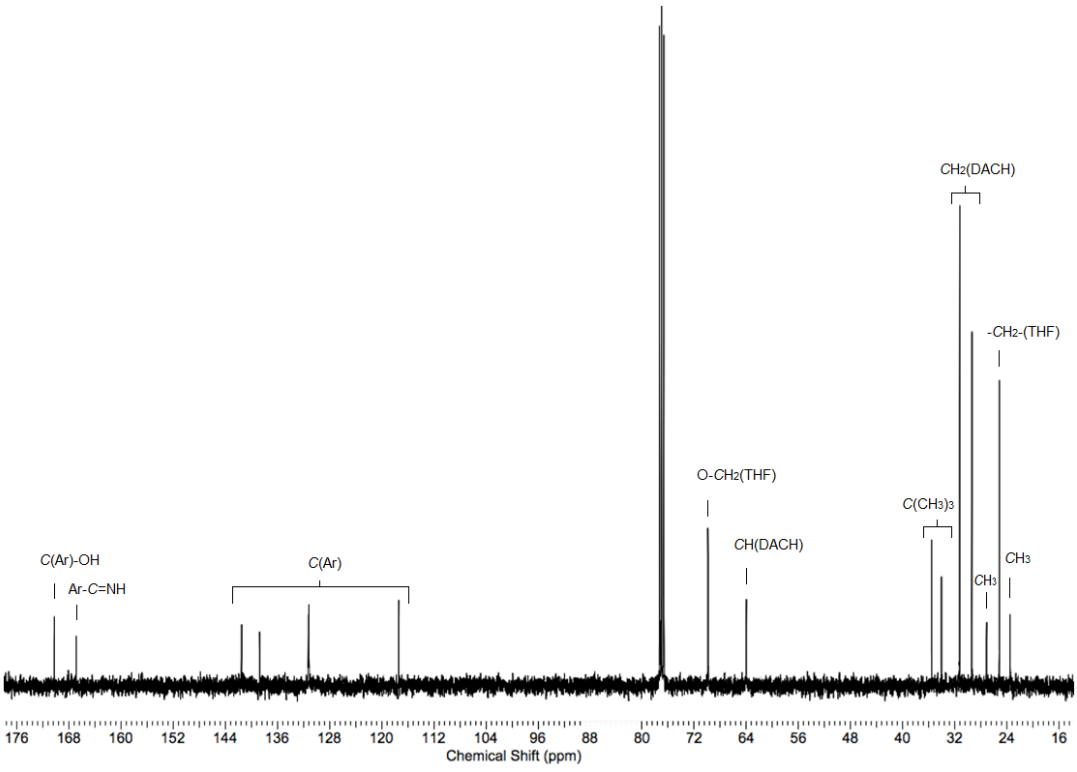

(S1c)

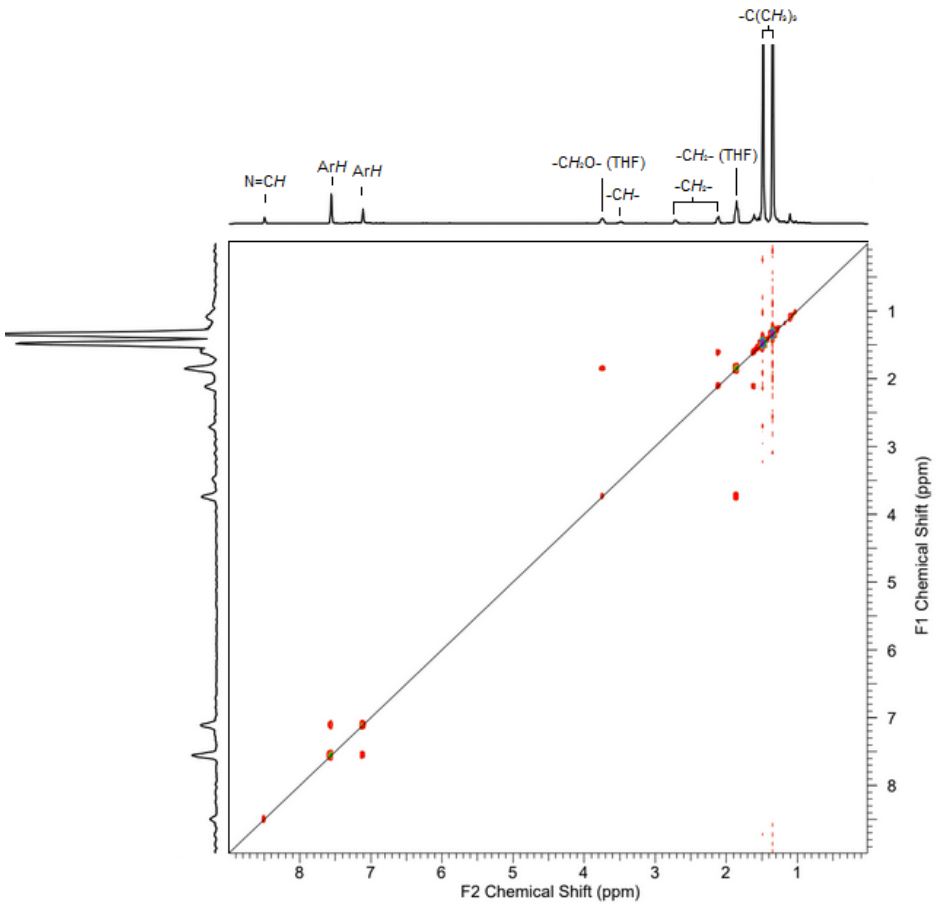

Figure S1 (a) ^{1}H NMR, (b) $^{13}C\{^{1}H\}$ NMR and (c) ^{1}H-^{1}H COSY spectrum of $[(ONNO)In(THF)_2][SbF_6]$ (**3**). Spectral features of (**1**) and (**2**) are identical. (400 MHz, $CDCl_3$, 25 °C).

(S2a)

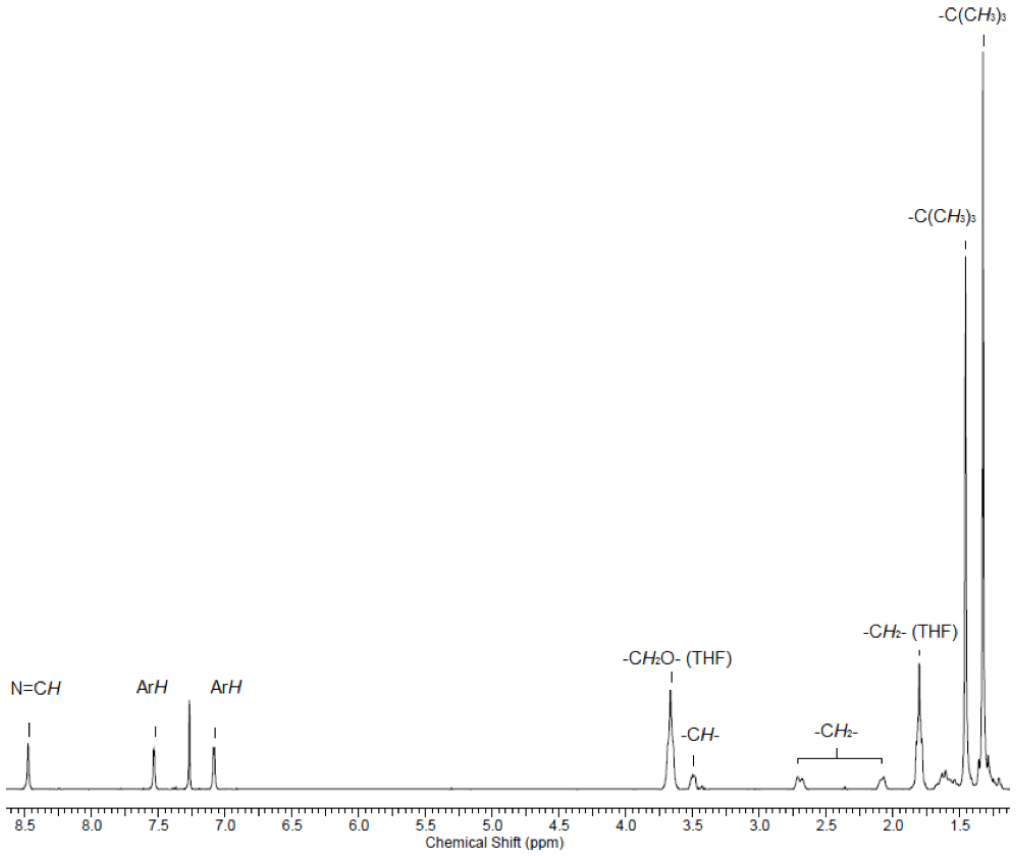
-C(CH3)3
-C(CH3)3
-CH2- (THF)
-CH2O- (THF)
N=CH
ArH
ArH
-CH-
-CH2-
8.5
8.0
7.5
7.0
6.5
6.0
5.5
5.0
4.5
4.0
3.5
3.0
2.5
2.0
1.5
Chemical Shift (ppm)

(S2b)

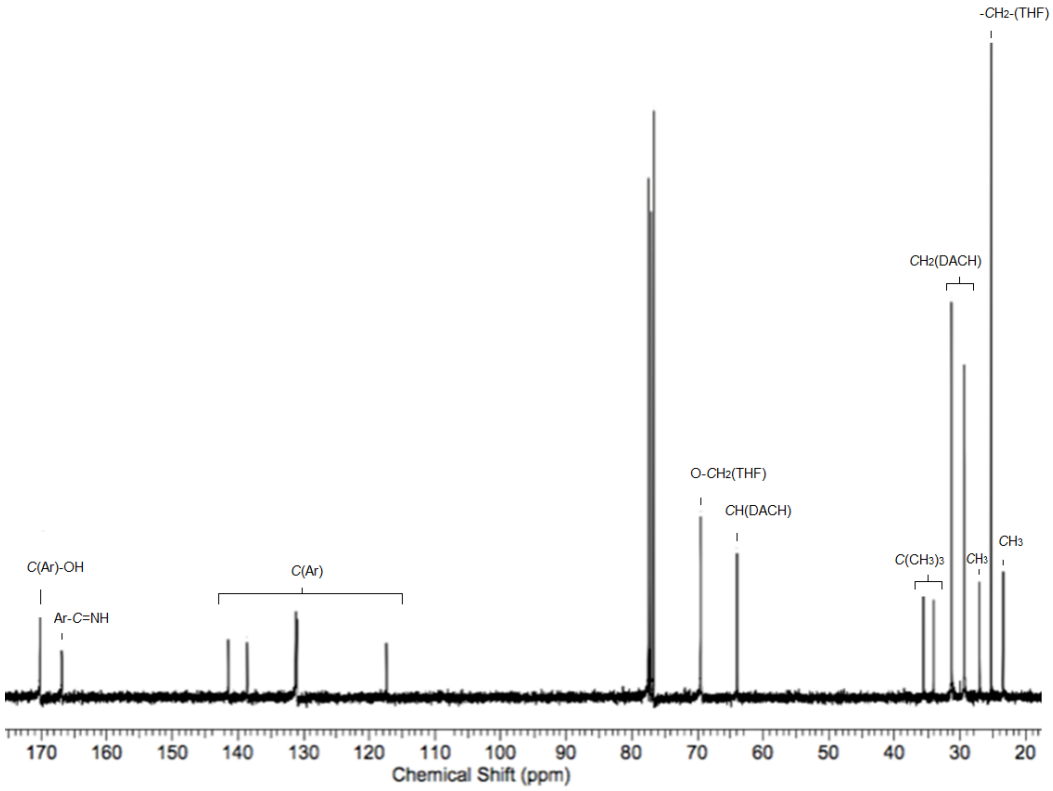
-CH2-(THF)
CH2(DACH)
O-CH2(THF)
CH(DACH)
C(Ar)-OH
Ar-C=NH
C(Ar)
C(CH3)3
CH3
CH3
170
160
150
140
130
120
110
100
90
80
70
60
50
40
30
20
Chemical Shift (ppm)

Figure S2 (a) ^{1}H NMR and (b) $^{13}C\{^{1}H\}$ NMR spectrum of $[(ONNO)In(THF)_2][PF_6]$ (**1**).

(S3a)

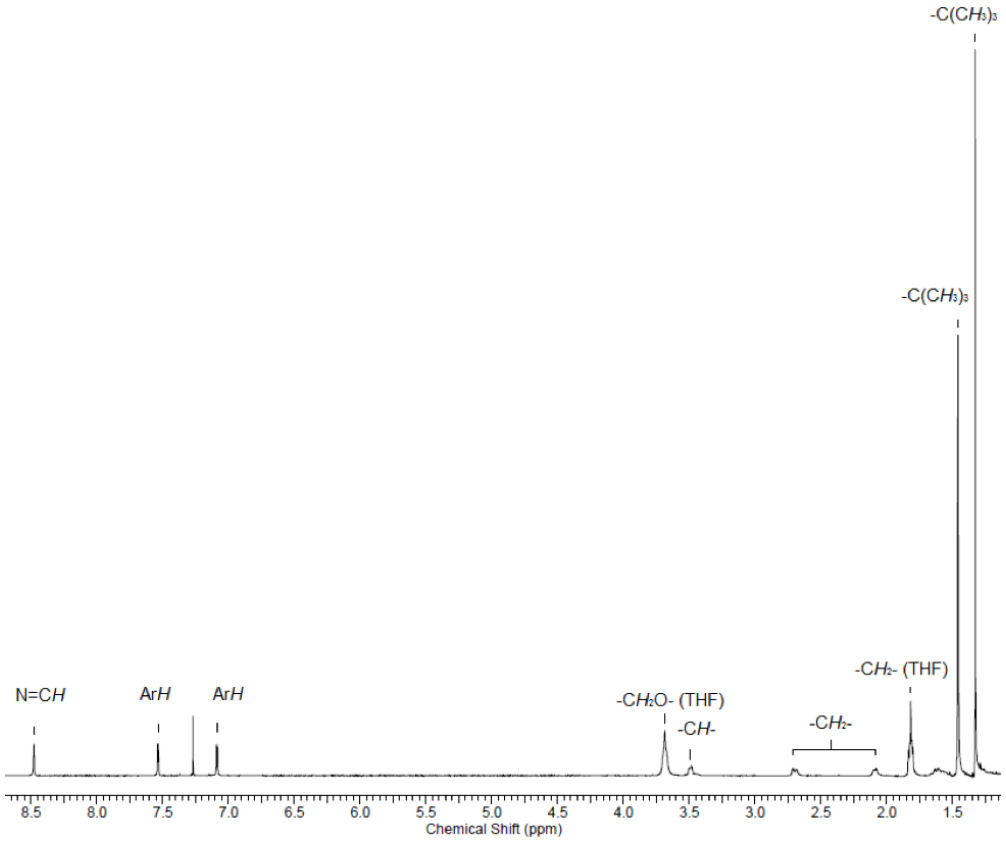

(S3b)

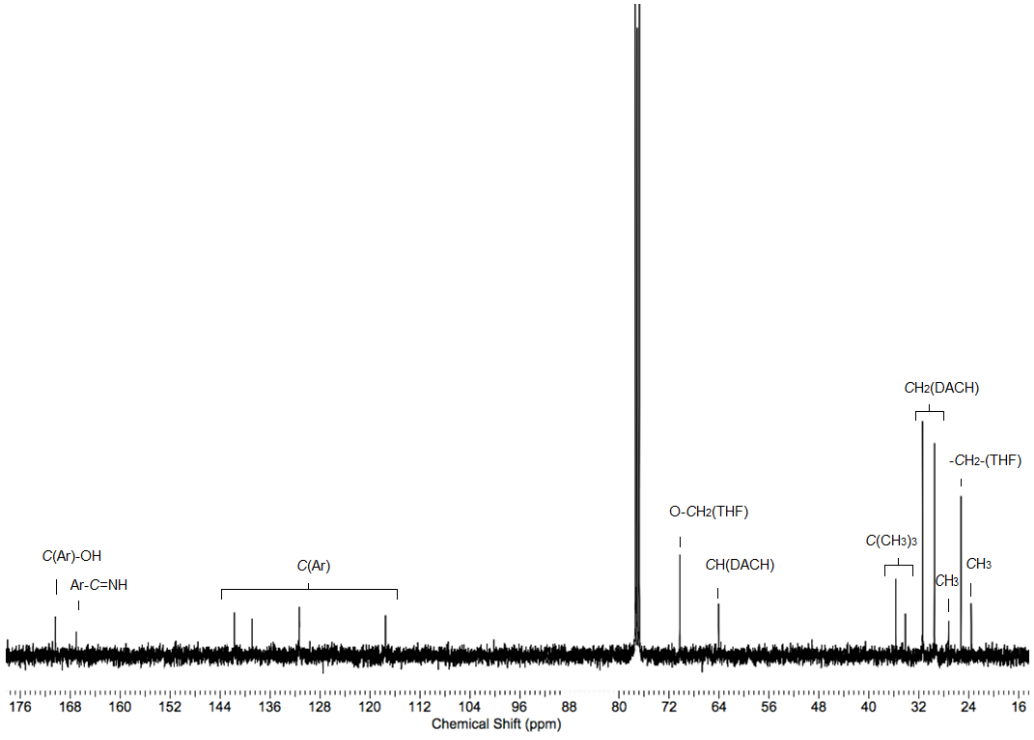

Figure S3 (a) ^{1}H NMR and (b) $^{13}C\{^{1}H\}$ NMR spectrum of $[(ONNO)In(THF)_2][AsF_6]$ (**2**).

(S4a)

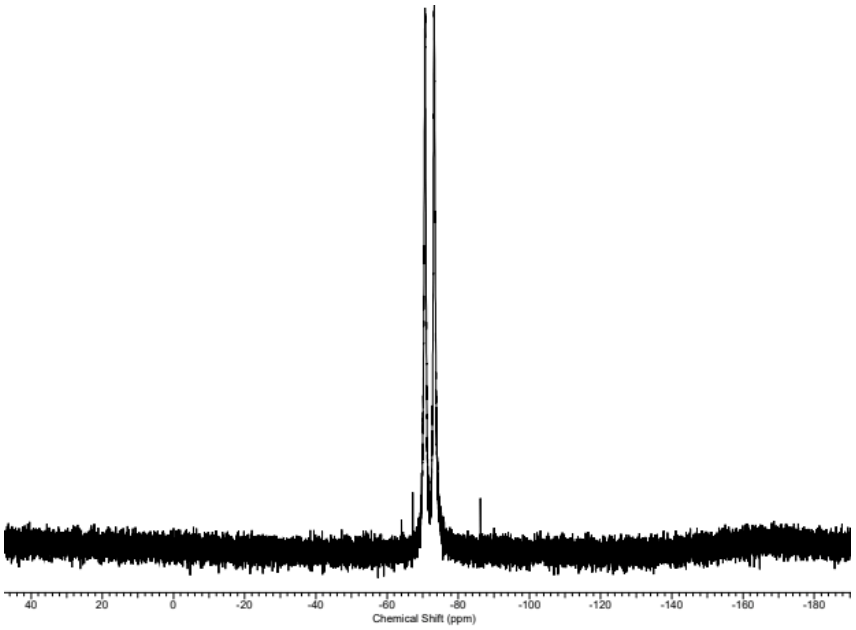

(S4b)

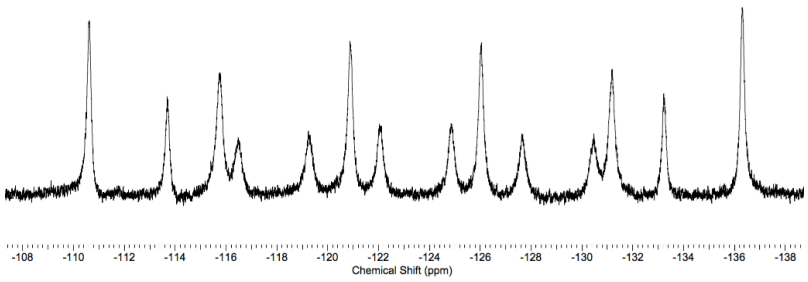

Figure S4. $^{19}F\{^{1}H\}$ NMR spectra of (a) $[(ONNO)In(THF)_2][PF_6]$ ($CDCl_3$, 25 °C) (**1**) and (b) $[(ONNO)In(THF)_2][SbF_6]$ (**3**) (CD_3CN, 25 °C).

(S5a)

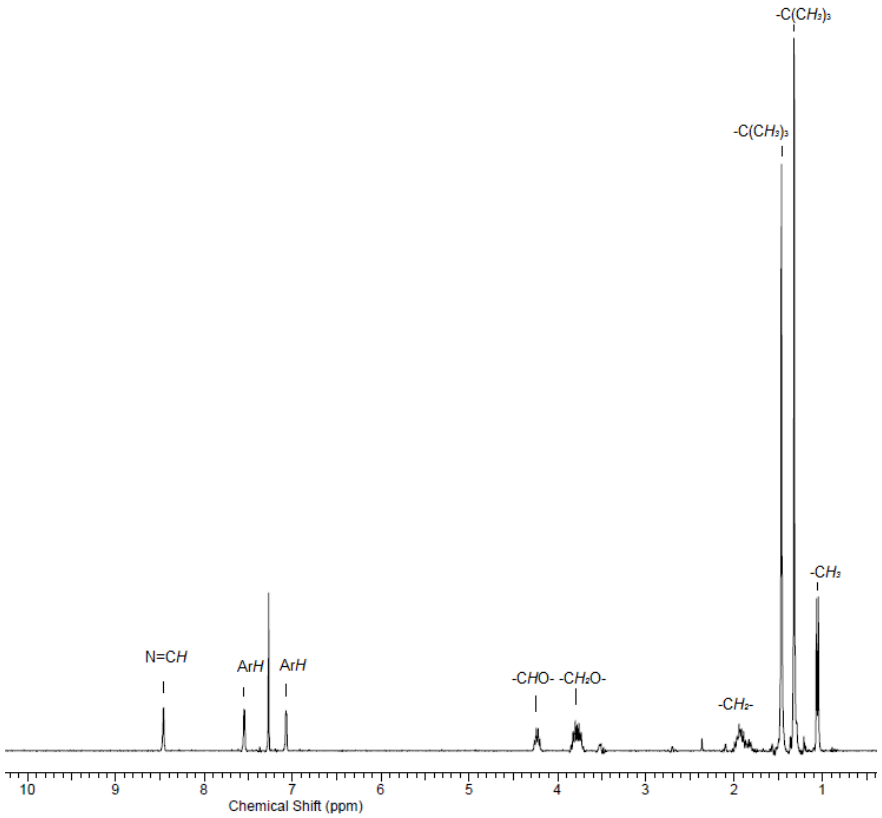
-C(CH3)3
-C(CH3)3
-CH2
N=CH
ArH
ArH
-CHO- -CH2O-
-CH2-
10
9
8
7
6
5
4
3
2
1
Chemical Shift (ppm)

(S5b)

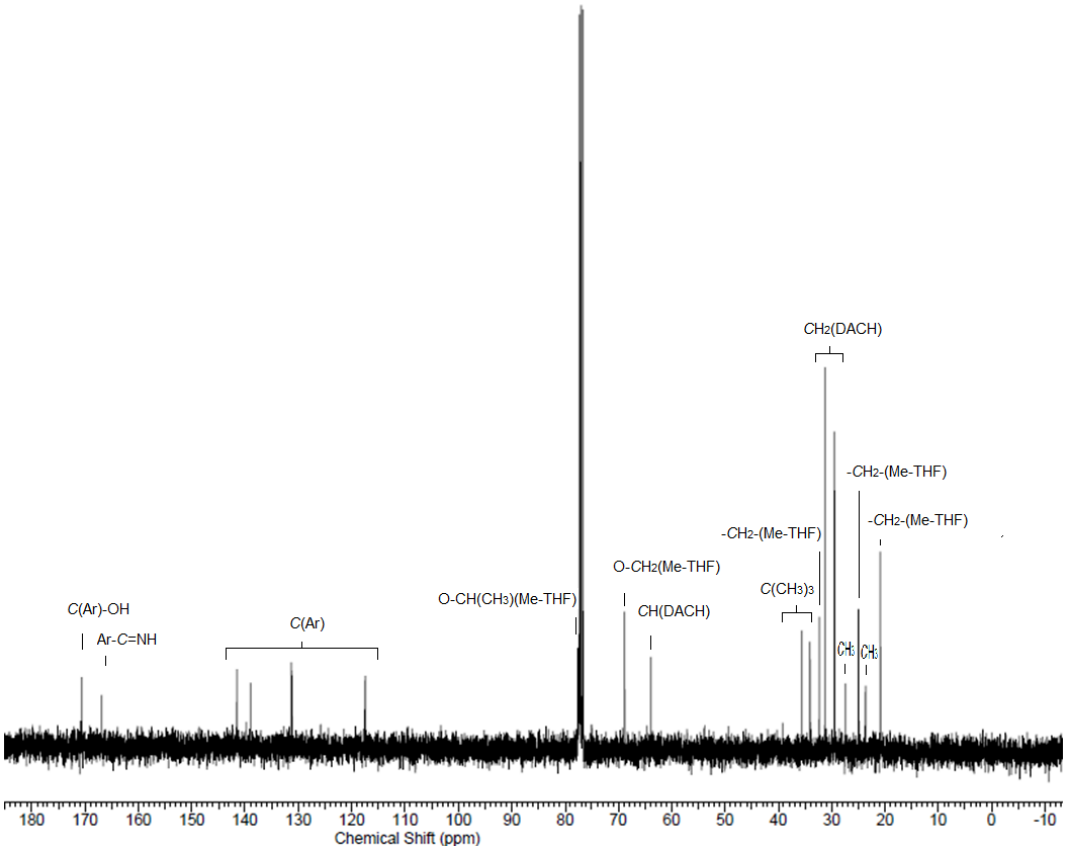
CH2(DACH)
-CH2-(Me-THF)
-CH2-(Me-THF)
-CH2-(Me-THF)
O-CH2(Me-THF)
C(CH3)3
C(Ar)-OH
Ar-C=NH
C(Ar)
O-CH(CH3)(Me-THF)
CH(DACH)
180
170
160
150
140
130
120
110
100
90
80
70
60
50
40
30
20
10
0
-10
Chemical Shift (ppm)

(S5c)

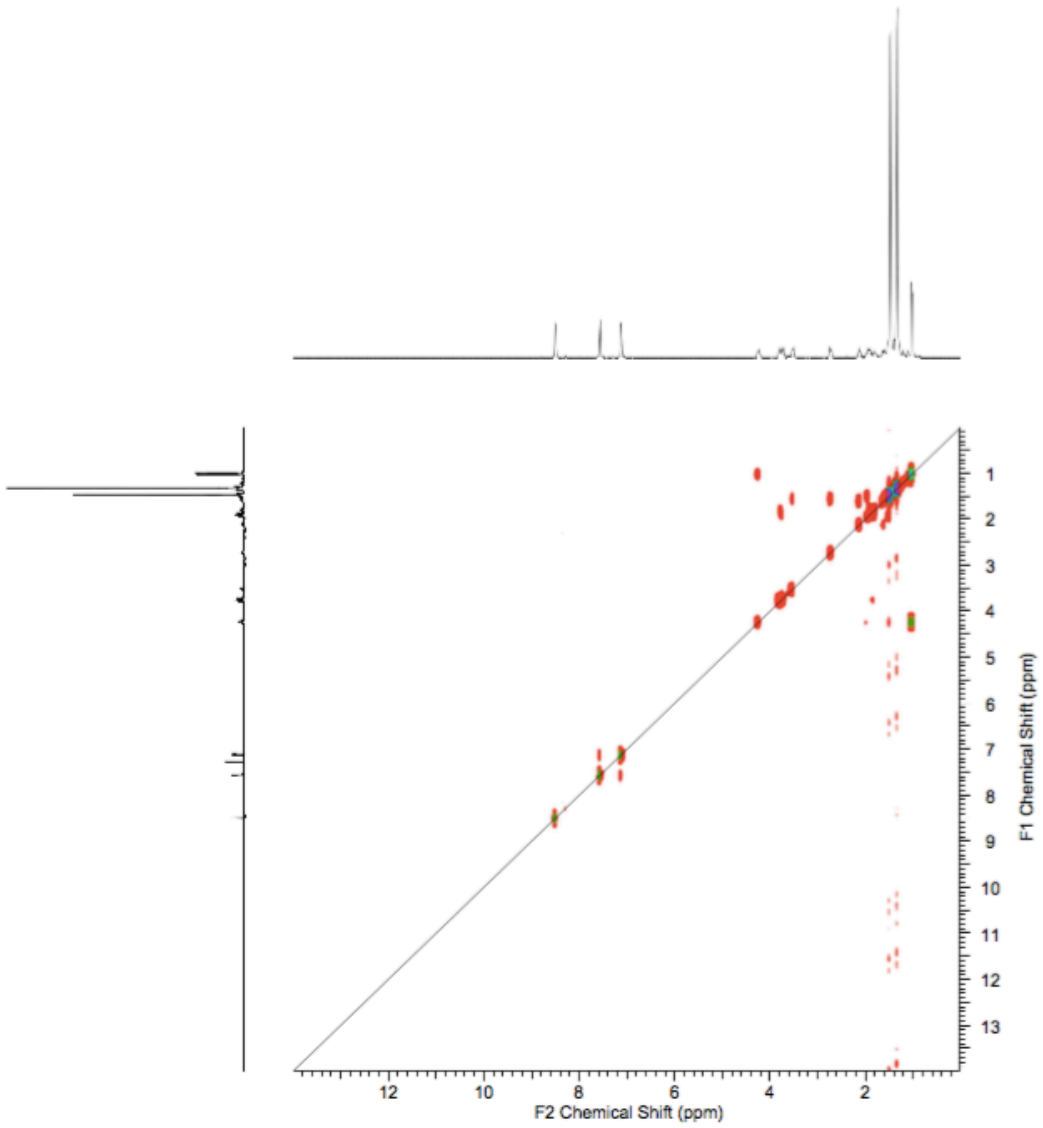

Figure S5. (a) ^{1}H NMR, (b) ^{13}C{^{1}H} NMR and (c) ^{1}H-^{1}H COSY spectrum of [(ONNO)In(Me-THF)$_2$][SbF$_6$] (**5**). (400 MHz, CDCl$_3$, 25 °C).

(S6a)

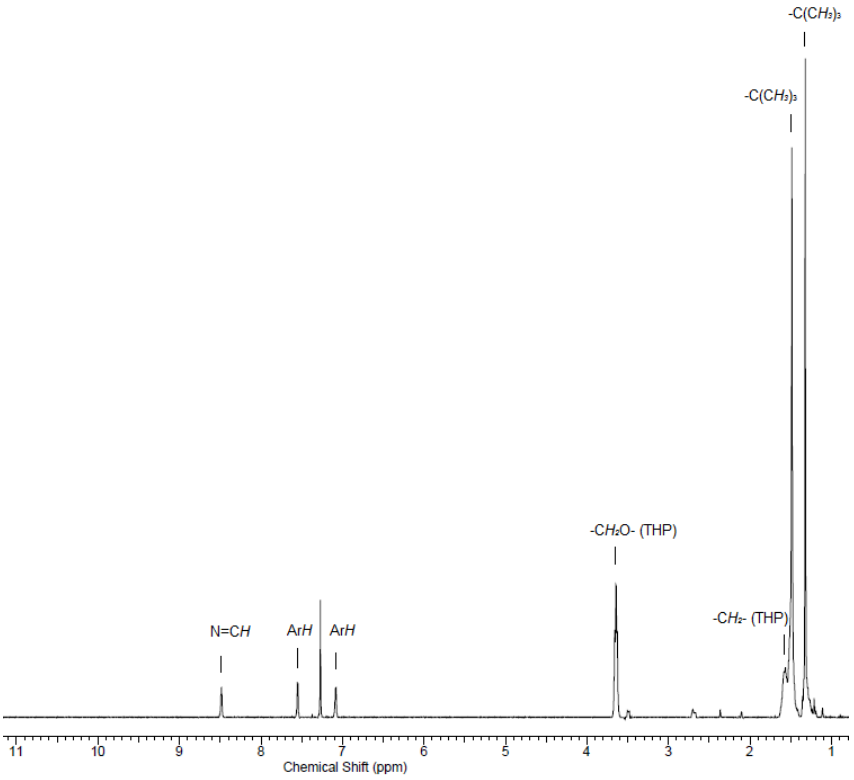
-C(CH3)3
-C(CH3)3
-CH2O- (THP)
-CH2- (THP)
N=CH
ArH
ArH
11
10
9
8
7
6
5
4
3
2
1
Chemical Shift (ppm)

(S6b)

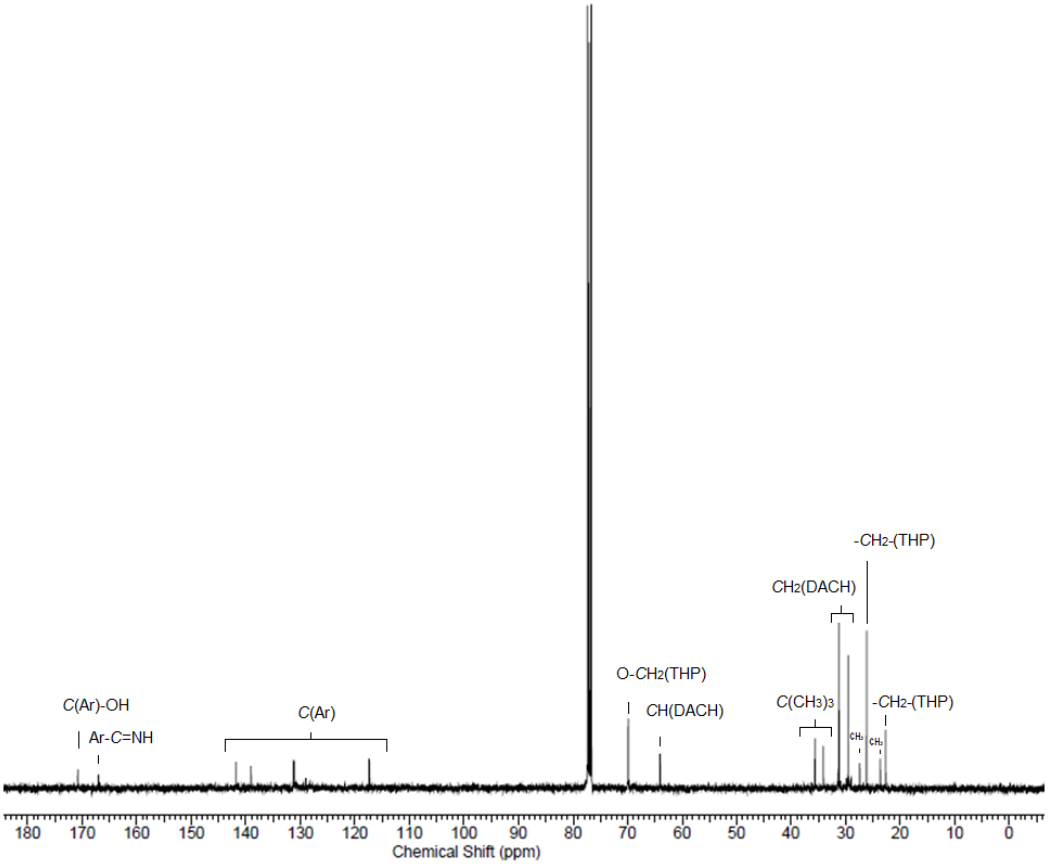
-CH2-(THP)
CH2(DACH)
O-CH2(THP)
C(Ar)-OH
C(Ar)
CH(DACH)
C(CH3)3
-CH2-(THP)
Ar-C=NH
180
170
160
150
140
130
120
110
100
90
80
70
60
50
40
30
20
10
0
Chemical Shift (ppm)

(S6c)

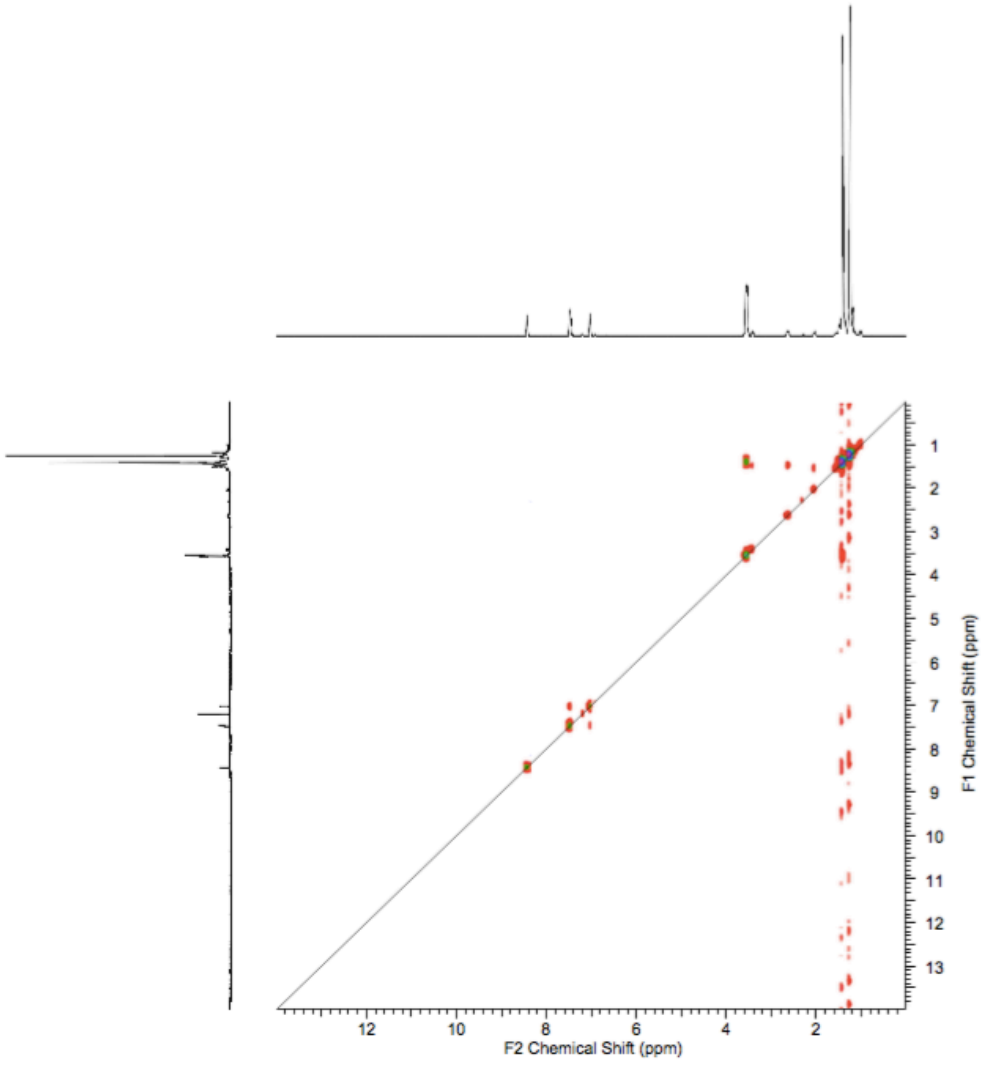

Figure S6 (a) ^{1}H NMR, (b) $^{13}C\{^{1}H\}$ NMR and (c) ^{1}H-^{1}H COSY spectrum of $[(ONNO)In(THP)_2][SbF_6]$ (**6**). (400 MHz, $CDCl_3$, 25 °C).

C. Characterization of complexes in the solid state

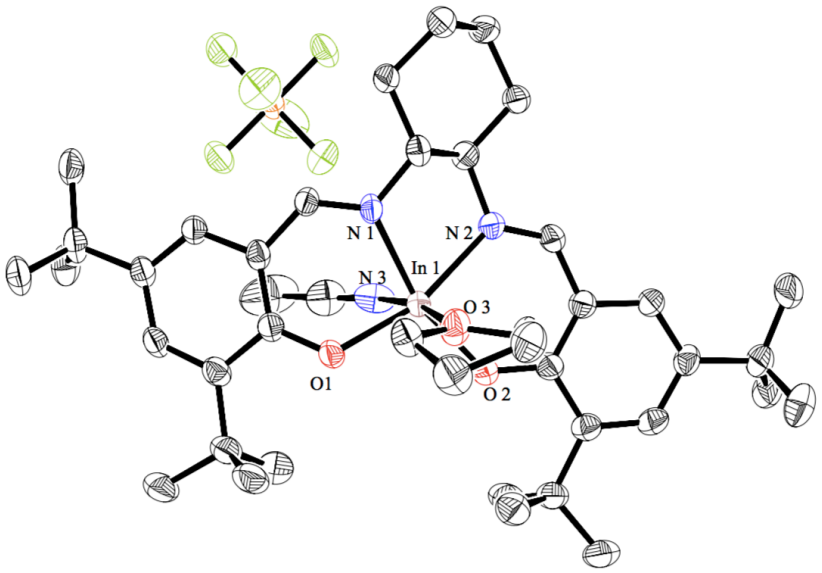

Selected bond length (Å) and angles (°) for complex **(1')**.				
Bond Lengths	In1-O1	2.061(2)	In1-O3	2.260(2)
	In1-N1	2.169(3)	In1-N3	2.353(6)
Bond Angles	N1-In1-O3	86.30(9)	O3-In1-N3	169.9(2)

Figure S7. Molecular structure of complex [(ONNO)In(ACN)(THF)][PF_6] (**1'**) (With ellipsoids at 50% probability and H atoms removed for clarity).

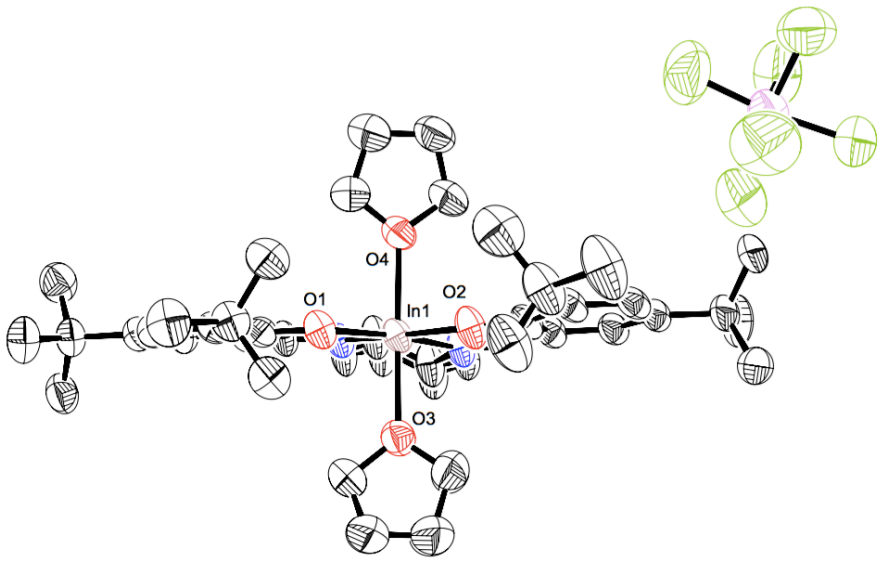

Selected bond length (Å) and angles (°) for complex **(3)**.				
Bond Lengths	In1-O1	2.041(5)	In1-O3	2.287(6)
	In1-N1	2.173(6)	In1-O4	2.287(5)
Bond Angles	N1-In1-O3	88.8(2)	O3-In1-O4	176.5(2)

Figure S8. Molecular structure of complex $[(ONNO)In(THF)_2][SbF_6]$ (**3**) (With ellipsoids at 30% probability and H atoms removed for clarity).

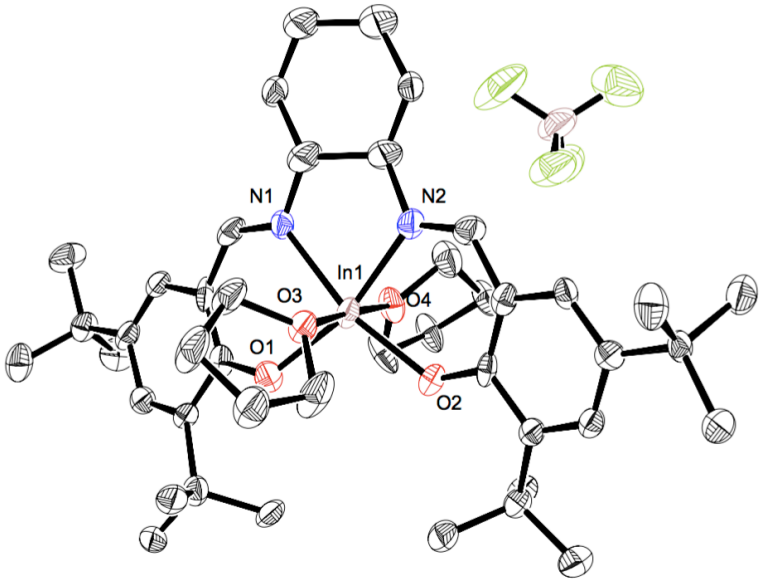

Selected bond length (Å) and angles (°) for complex **(4)**.				
Bond Lengths	In1-O1	2.042(3)	In1-O4	2.267(4)
	In1-N1	2.146(5)	In1-O3	2.272(3)
Bond Angles	N1-In1-O3	87.83(16)	O3-In1-O4	177.34(14)

Figure S9. Molecular structure of complex $[(ONNO)In(THF)_2][BF_4]$ (**4**) (With ellipsoids at 50% probability and H atoms removed for clarity).

Table S1. Selective crystal data for 3, 4, and 1'.

	3	4	1'
empirical formula	$C_{44}H_{68}InN_2O_4SbF_6$	$C_{48}H_{76}InN_2O_5BF_4$	$C_{49}H_{72}InN_3O_3PF_6$
fw	1039.57	962.73	1013.63
T (K)	100(2)	100(2)	100(2)
a (Å)	27.115(3)	9.2636(12)	38.279(5)
b (Å)	10.3591(9)	15.978(2)	15.4120(19)
c (Å)	41.932(4)	16.814(2)	17.904(2)
α (deg)	90	78.475(5)	90
β (deg)	102.098(6)	85.242(5)	100.866(4)
γ (deg)	90	82.119(5)	90
volume (Å^3)	11517(2)	2411.7(6)	10373(2)
Z	8	2	8
cryst syst	monoclinic	triclinic	monoclinic
space group	C2/c	P -1	C2/c
d_{calc} (g/cm^3)	1.199	1.326	1.298
μ (Mo Kα) (cm^{-1})	9.22	5.44	5.42
$2\theta_{max}$ (deg)	44.956	47.18	55.22
absor corr (T_{min}, T_{max})	0.666, 0.746	0.673, 0.745	0.388, 0.746
total no. of reflns	60 629	15 110	51 203
no. of indep reflns (R_{int})	7517 (0.0503)	6 891 (0.0528)	11 949 (0.0772)
residuals (refined on F^2): R_1; wR_2	0.1601, 0.3220	0.0871, 0.1733	0.0699, 0.1763
GOF	1.031	1.002	1.030
no. obsrvns [$I > 2\sigma(I)$]	13282	6099	11 949
residuals (refined on F^2: R_1[a]; wR_2[b])	0.0816, 0.2676	0.0578, 0.1421	0.0578, 0.1670

[a] $R_1 = \Sigma \, ||F_o| - |F_c|| \, / \Sigma \, |F_o|$. [b] $wR_2 = [\, \Sigma \, (\, w \, (F_o^2 - F_c^2)^2 \,) / \, \Sigma \, w(F_o^2)_2]^{1/2}$

D. ROP of cyclic ethers and esters

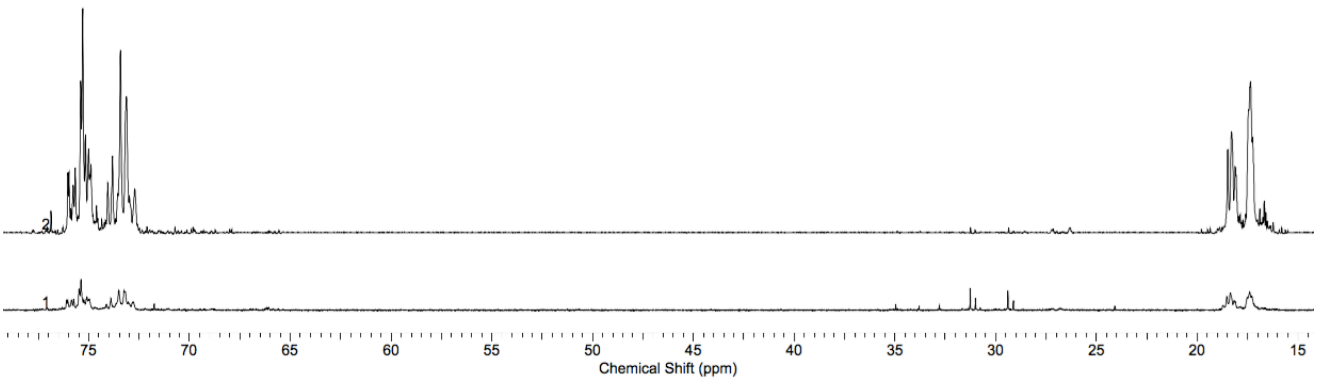

Figure S10. Methine and methylene regions of the $^{13}C\{^{1}H\}$ spectrum of the isolated products from the ROP of racemic propylene oxide in neat conditions at 25 °C with **3** (bottom) and with (*R,R*)-**3** (top). (101 MHz, $CDCl_3$, 25 °C).

Table S2. Copolymerization of cyclic ethers and epoxides with **3** in CD_2Cl_2 or C_6D_5Br at 25 °C.

	epoxide	Cyclic ether	[epox]/ [**3**]	[cyclic ether]/ [**3**]	time (h)	Solvent	Conv. epoxide (%)	Conv. cyclic ether (%)	isolated yield (%)	M_n theo (10^{-3} Da)	M_n (10^{-3} Da)	Mw (10^{-3} Da)	*Đ*
1	ECH	THF	10	100	48	CD_2Cl_2	32	19	0	-	-	-	-
2	1,2-epoxy-5-hexene	THF	10	100	48	CD_2Cl_2	99	0	0	-	-	-	-
3	ECH	THF	100	100	96	CD_2Cl_2	69	85	93	12.5	29.9	43.8	1.47
											21.4	28.4	1.33
4	1,2-epoxy-5-hexene	THF	100	100	96	CD_2Cl_2	90	80	86	14.6	17.8	24.7	1.38
											13.7	17.4	1.27
5	ECH	Oxetane	100	100	96	CD_2Cl_2	90	99	87	14.1	13.5	17.2	1.27
											10.4	17.6	1.69
6	ECH	Oxepane	100	100	96	C_6D_5Br	92	99	73	18.4	15.0	16.9	1.12
											11.4	13.9	1.22
7	-	Oxetane	0	100	24	CD_2Cl_2	-	99	66	5.7	13.1	20.6	1.58
8	-	Oxepane	0	100	24	C_6D_5Br	-	0	0	-	-	-	-
9	ECH	-	100	0	96	C_6D_5Br	99	-	45	9.2	4.0	6.6	1.33
											5.9	13.5	2.29

Reactions were performed in dichloromethane or bromobenzene at 25 °C. [cat] = 64.0 mM, [M2] = 6.4 M. aConversion was monitored by 1H NMR spectroscopy using 1,3,5-trimethoxybenzene as an internal standard. Molecular weights were determined by GPC measurements in THF. Theoretical molecular weights were calculated Calculated from [epox]o/[3] × epox conversion × Mepox + [cylic ether]$_o$/[**3**] × cyclic ether conversion × Mcyclic ether.

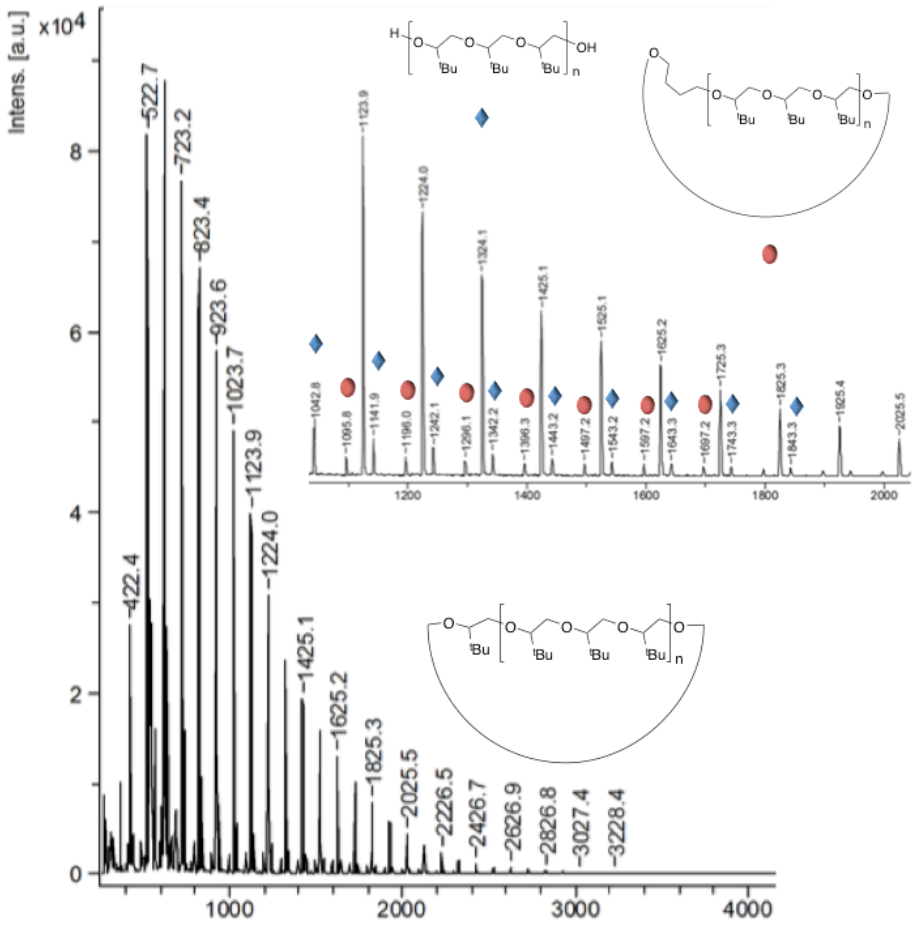

Figure S11. MALDI-TOF spectrum of the isolated product from the ROP of 1,2-epoxy-3,3-dimethylbutane with (3). The distributions refer to cyclic homopolymerization product, linear product with OH chain end and cyclic homopolymerization product with one ring-opened THF molecule.

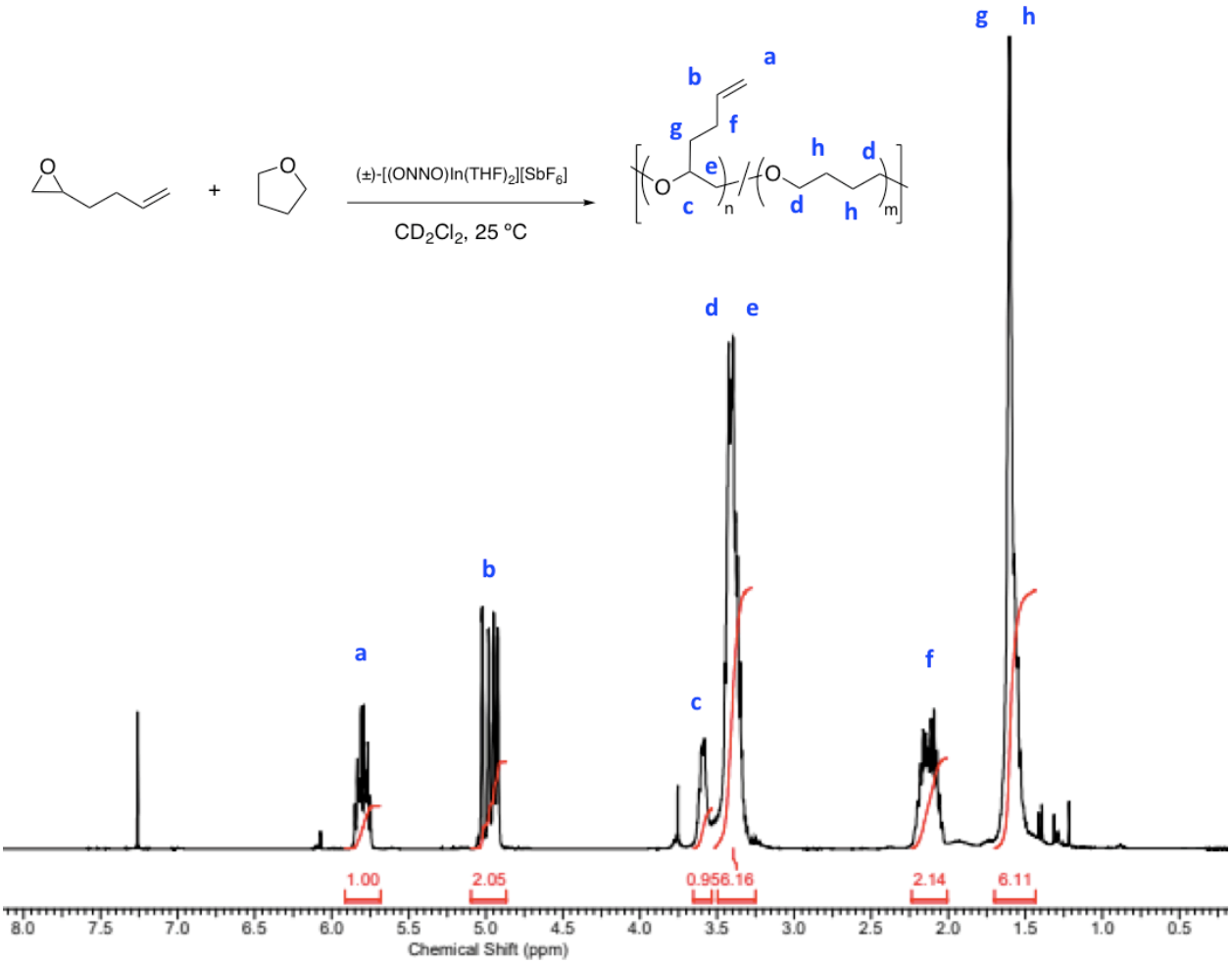

Figure S12. 1H NMR spectrum of the copolymerization product of THF and 1,2-epoxy-5-hexene (400 MHz, CDCl3, 25 °C).

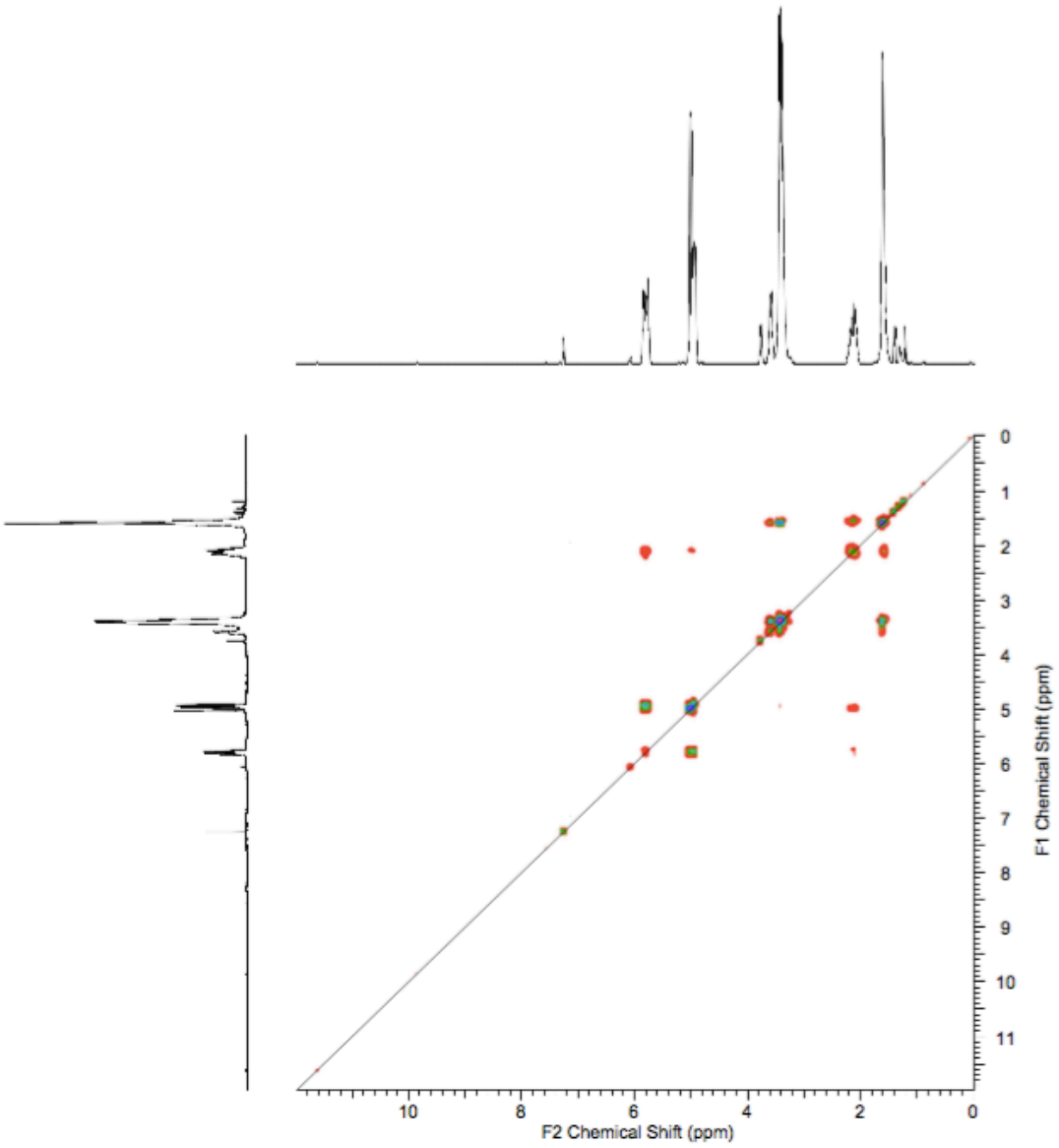

Figure S13. ^{1}H-^{1}H COSY spectrum of the copolymerization product of THF and 1,2-epoxy-5-hexene (400 MHz, $CDCl_3$, 25 °C).

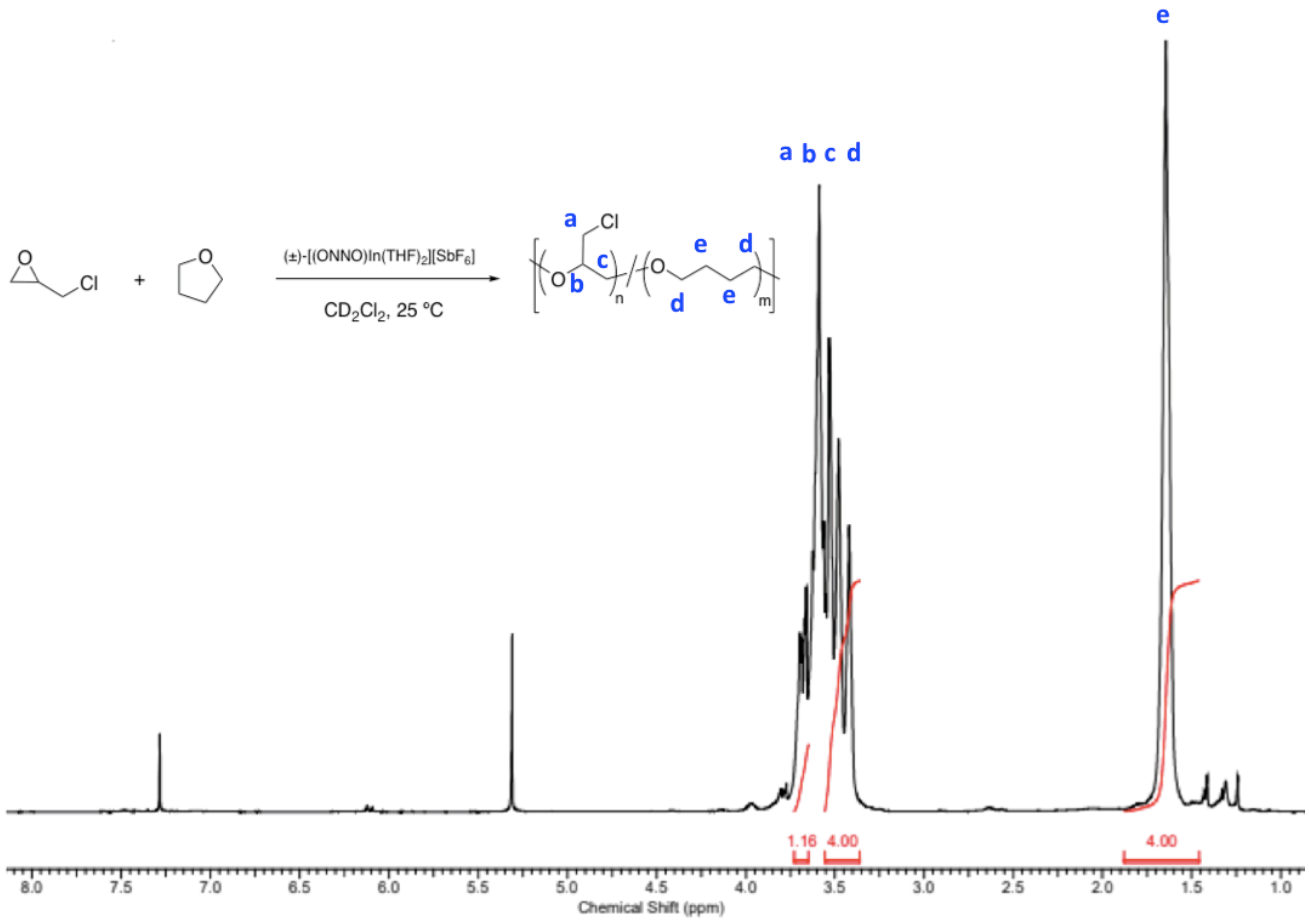

Figure S14. ^{1}H NMR spectrum of the copolymerization product of THF and epichlorohydrin (400 MHz, $CDCl_3$, 25 °C).

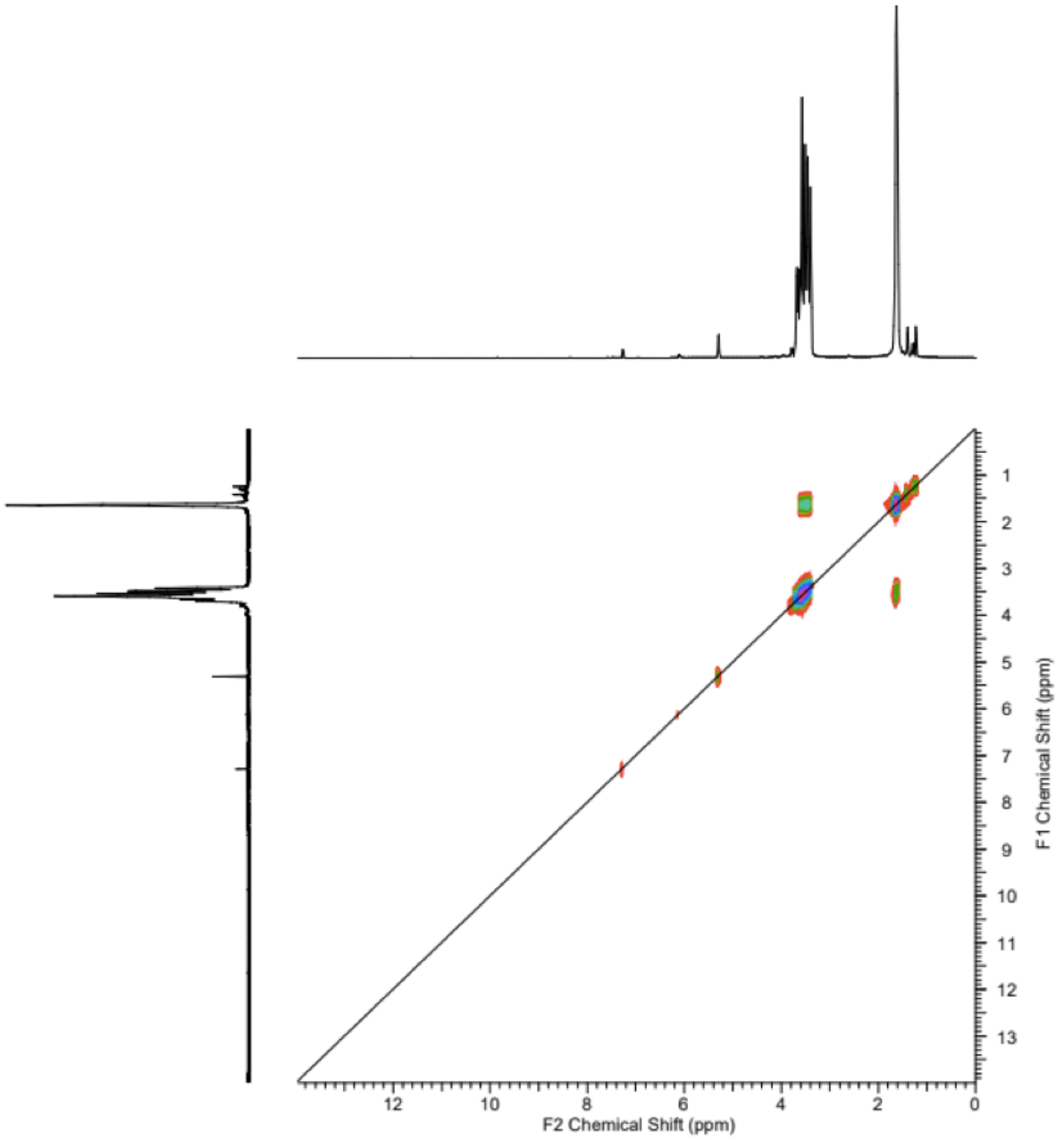

Figure S15. ^{1}H-^{1}H COSY spectrum of the copolymerization product of THF and epichlorohydrin (400 MHz, CDCl3, 25 °C).

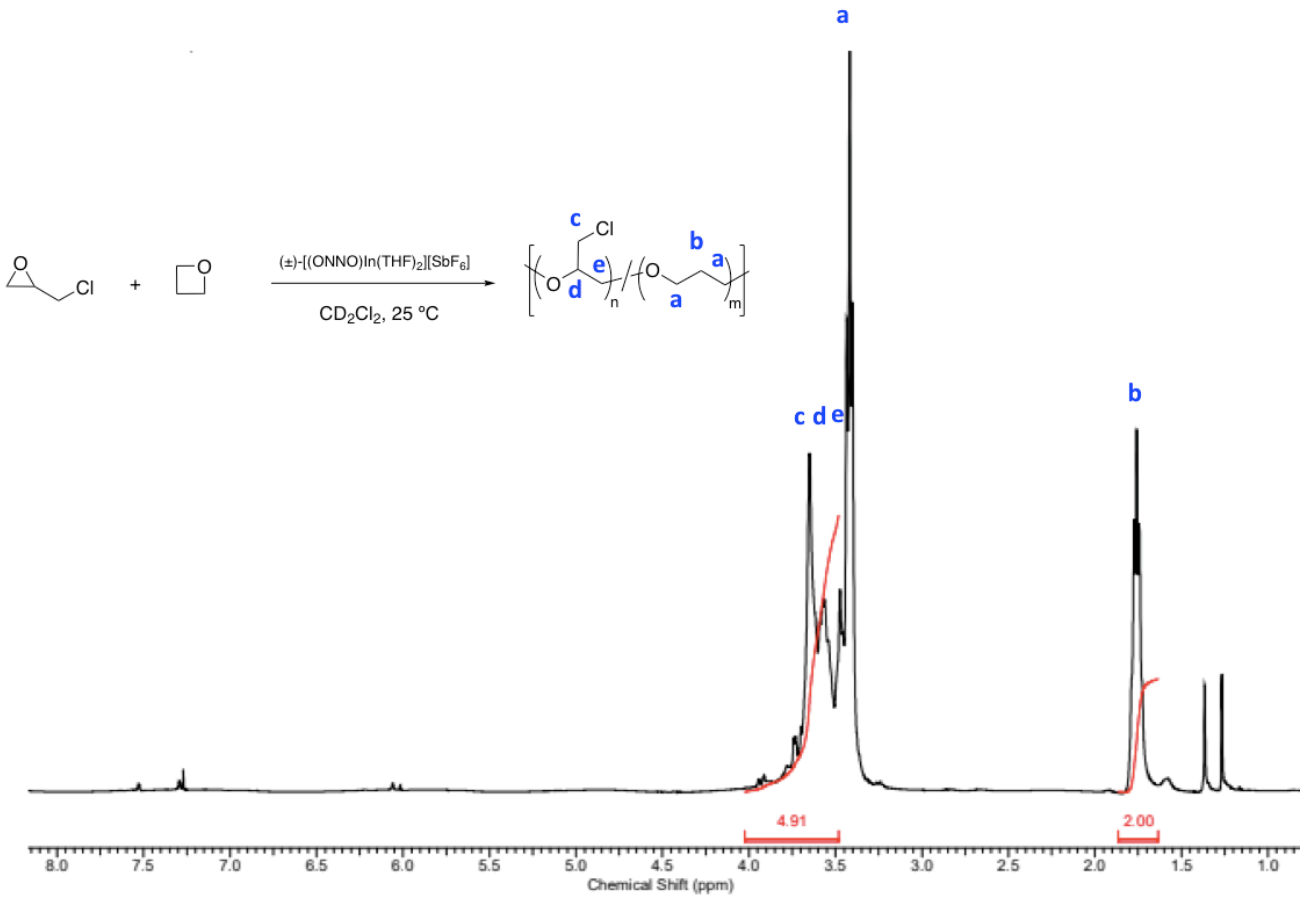

Figure S16. ^{1}H NMR spectrum of the copolymerization product of oxetane and epichlorohydrin (400 MHz, $CDCl_3$, 25 °C).

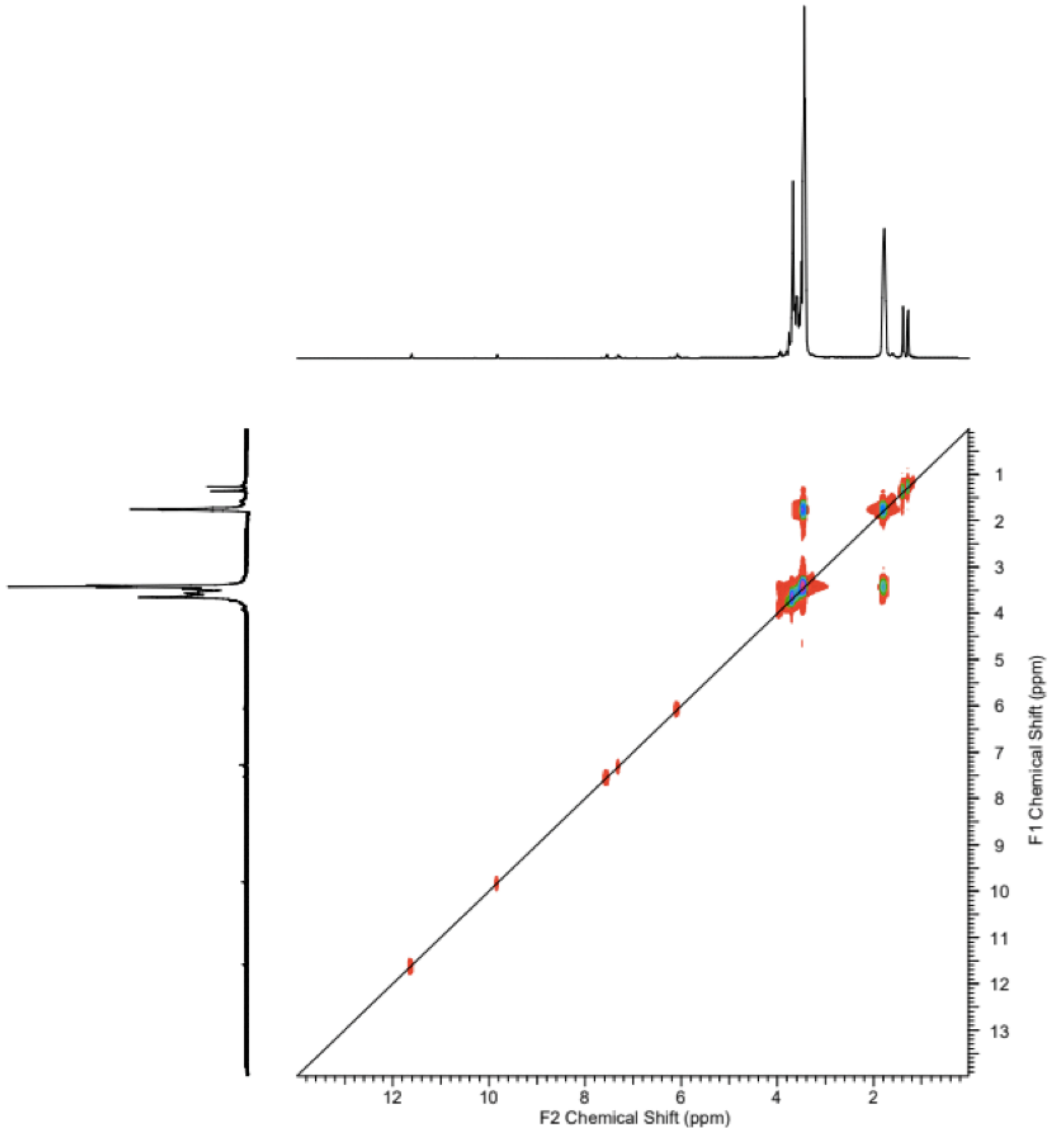

Figure S17. ^{1}H-^{1}H COSY spectrum of the copolymerization product of oxetane and epichlorohydrin (400 MHz, $CDCl_3$, 25 °C).

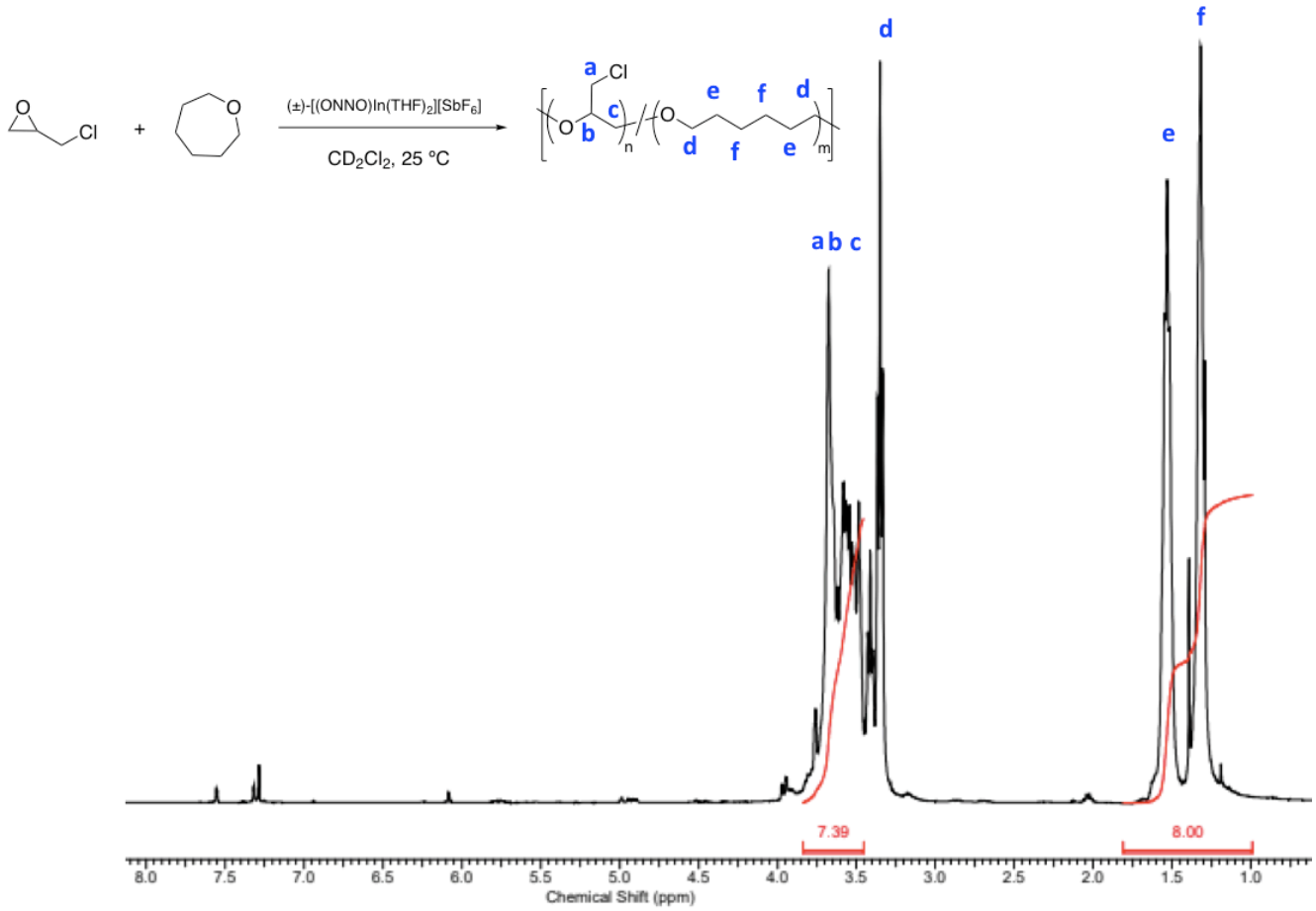

Figure S18. ^{1}H NMR spectrum of the copolymerization product of oxepane and epichlorohydrin (400 MHz, $CDCl_3$, 25 °C).

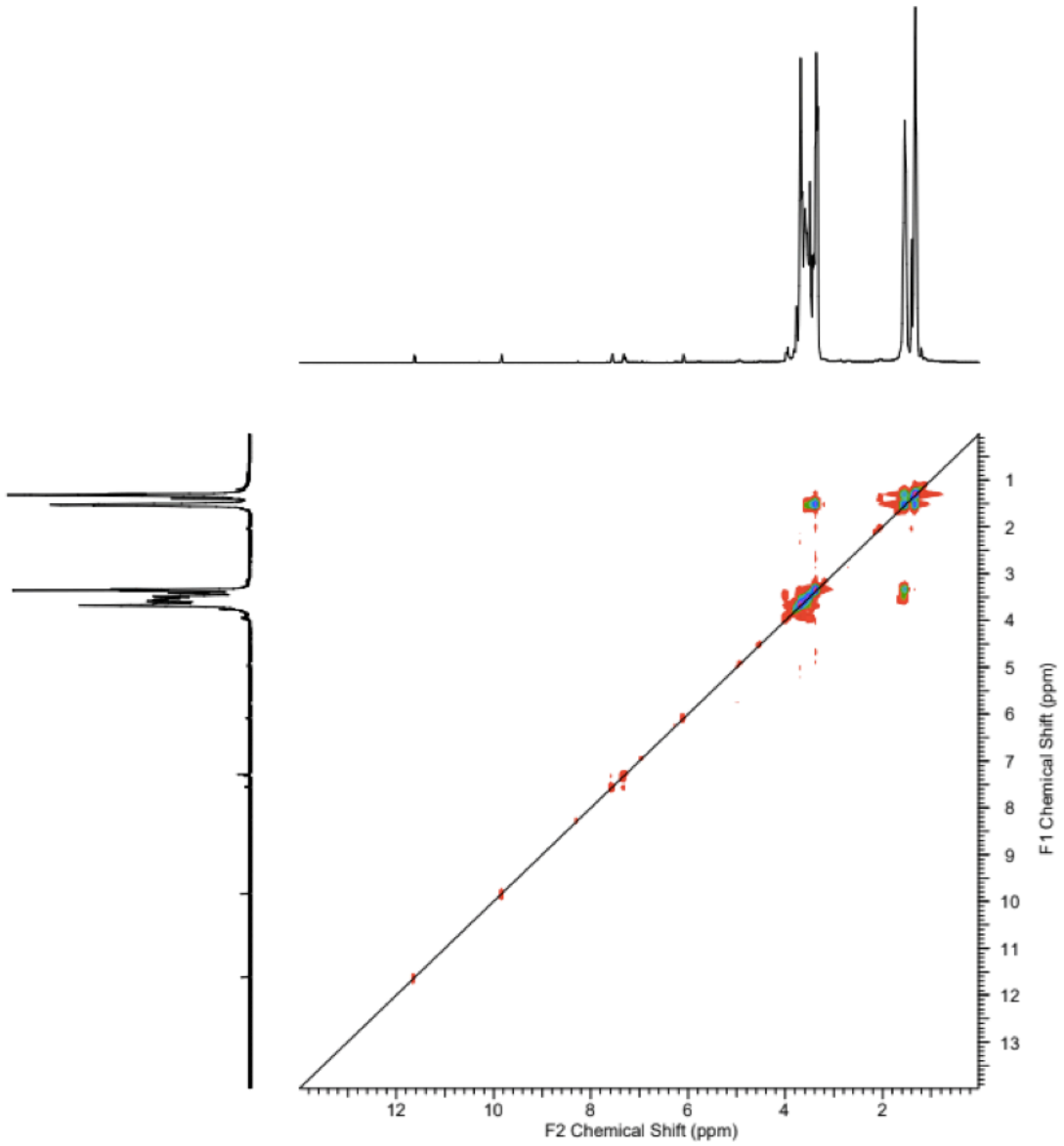

Figure S19. ^{1}H-^{1}H COSY spectrum of the copolymerization product of oxepane and epichlorohydrin (400 MHz, $CDCl_3$, 25 °C).

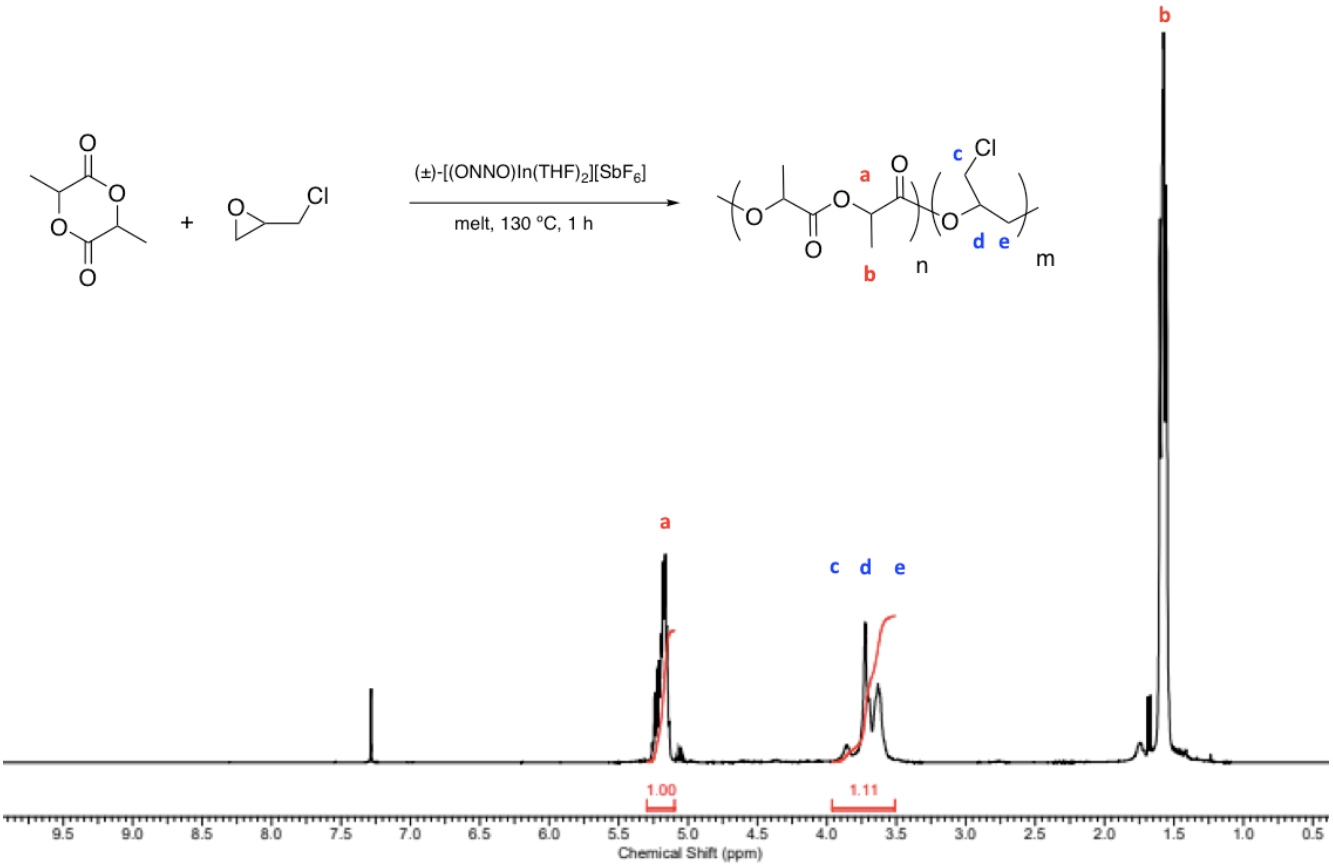

Figure S20. ^{1}H NMR spectrum of the copolymerization product of rac-lactide and epichlorohydrin (400 MHz, $CDCl_3$, 25 °C).

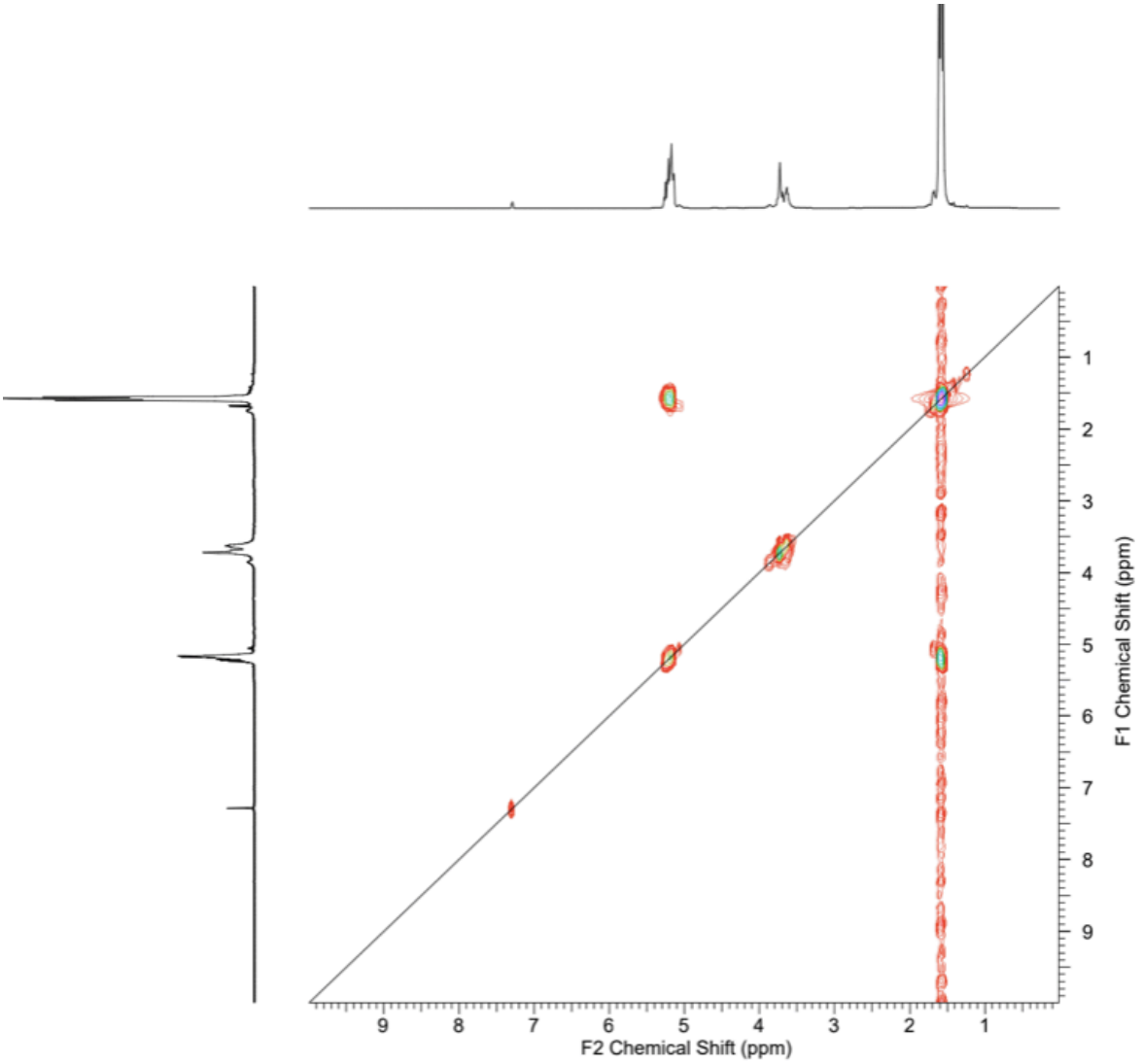

Figure S21. ^{1}H-^{1}H COSY spectrum of the copolymerization product of rac-lactide and epichlorohydrin (400 MHz, $CDCl_3$, 25 °C).

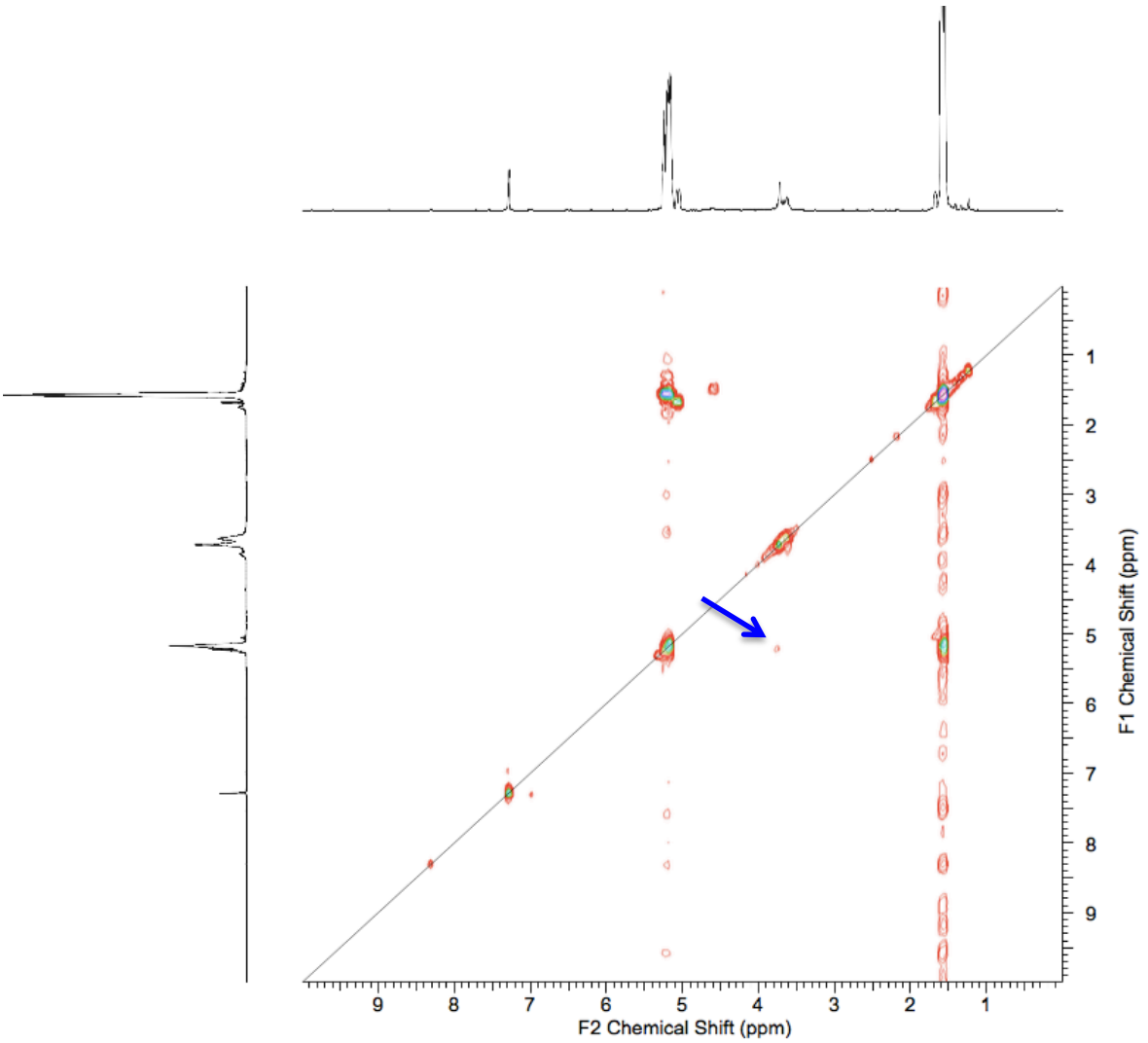

Figure S22. Long range ^{1}H-^{1}H COSY spectrum of the copolymerization product of rac-lactide and epichlorohydrin (400 MHz, $CDCl_3$, 25 °C).

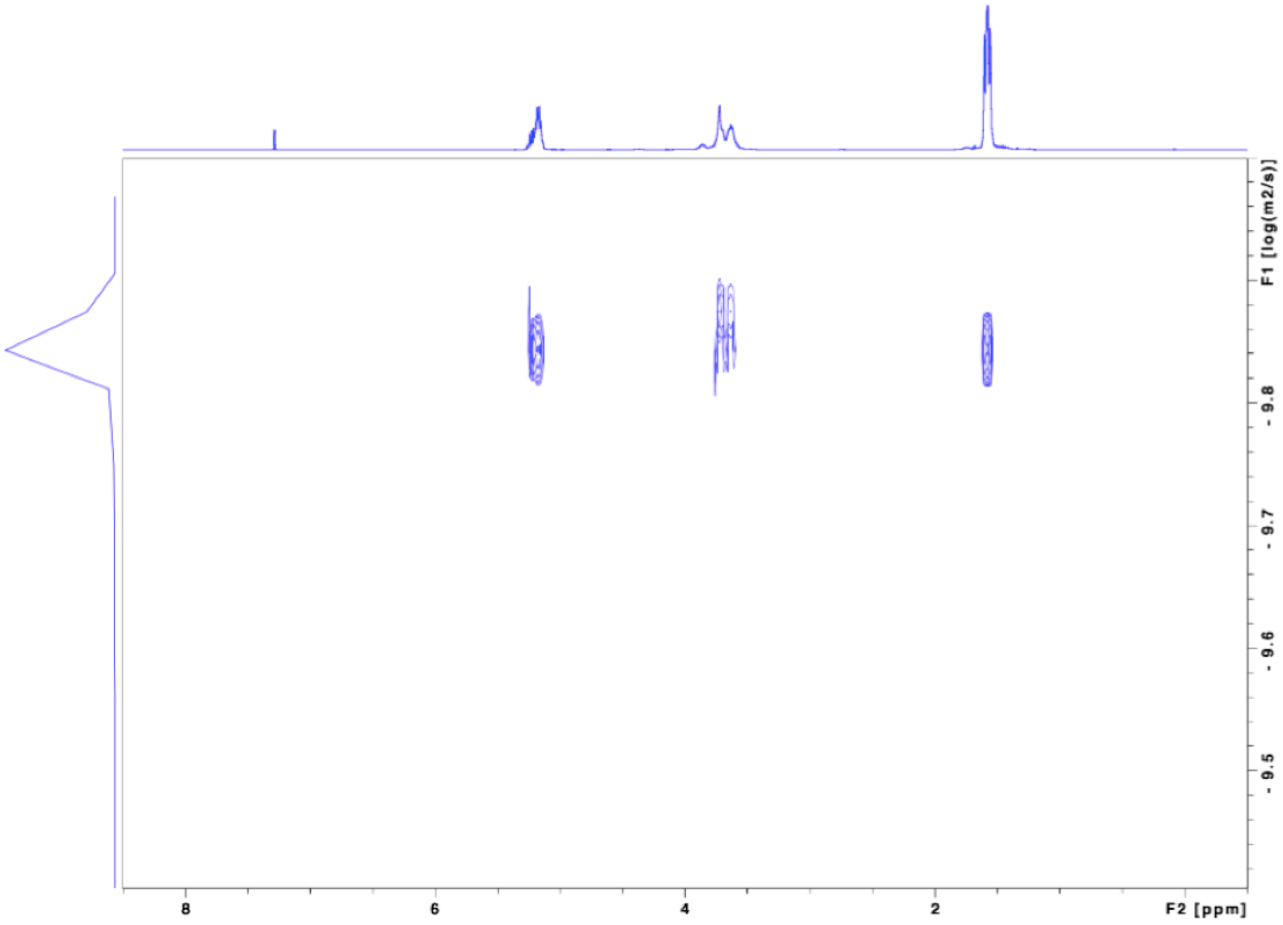

Figure S23. DOSY-NMR of the copolymerization product of rac-lactide and epichlorohydrin (400 MHz, $CDCl_3$, 25 °C).

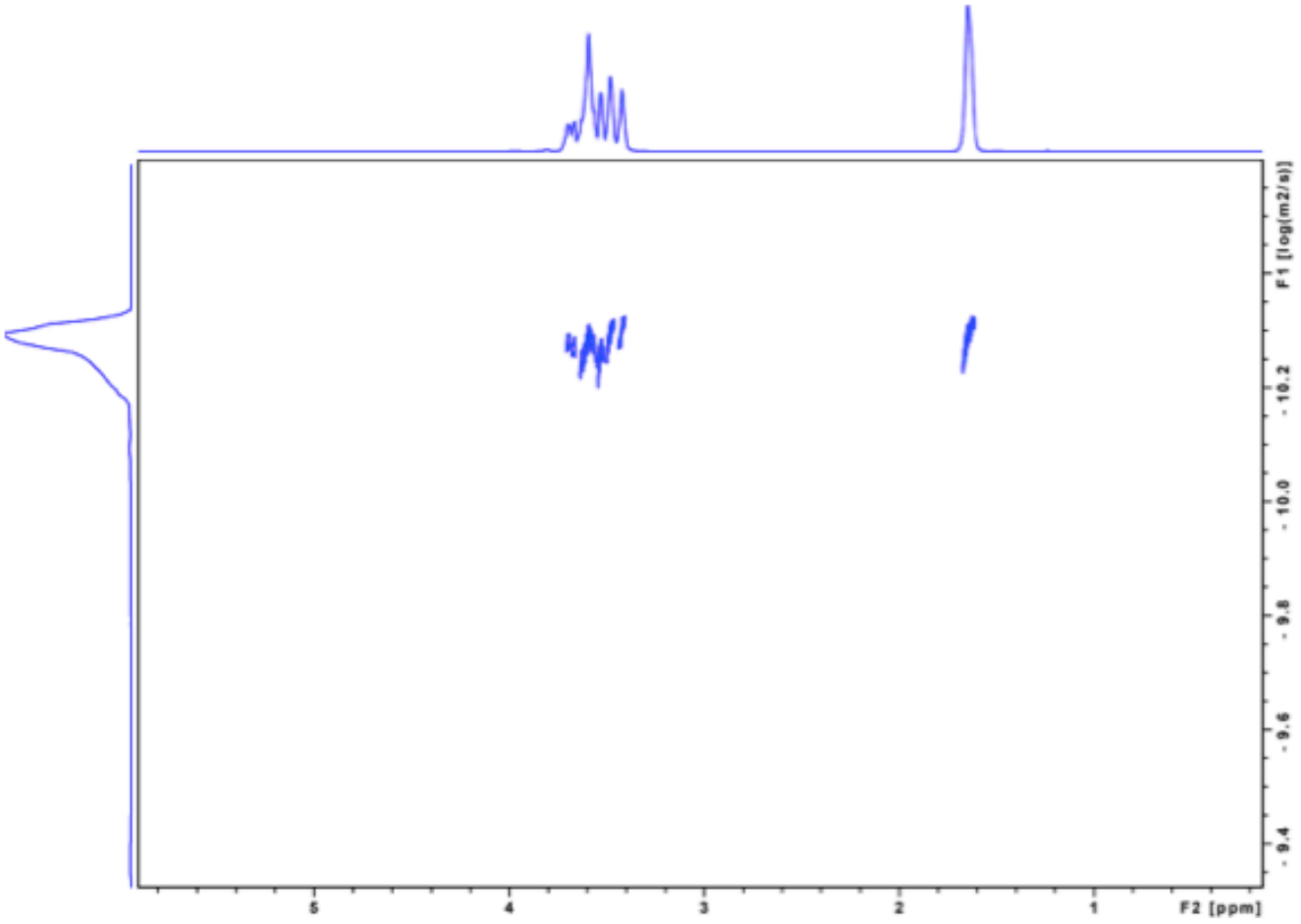

Figure S24. DOSY-NMR of the copolymerization product of tetrahydrofuran and epichlorohydrin (400 MHz, $CDCl_3$, 25 °C).

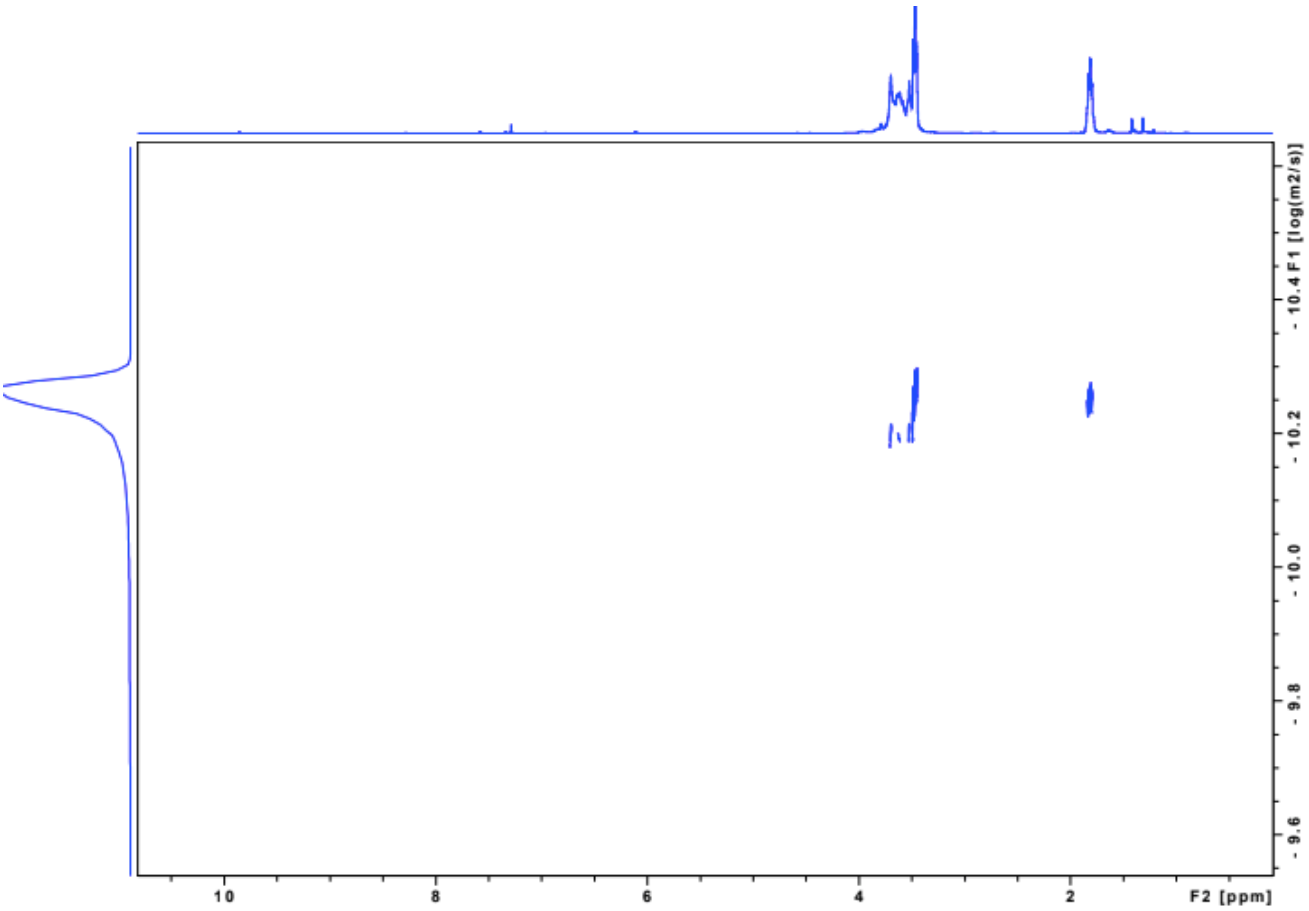

Figure S25. DOSY-NMR of the copolymerization product of oxetane and epichlorohydrin (400 MHz, $CDCl_3$, 25 °C).

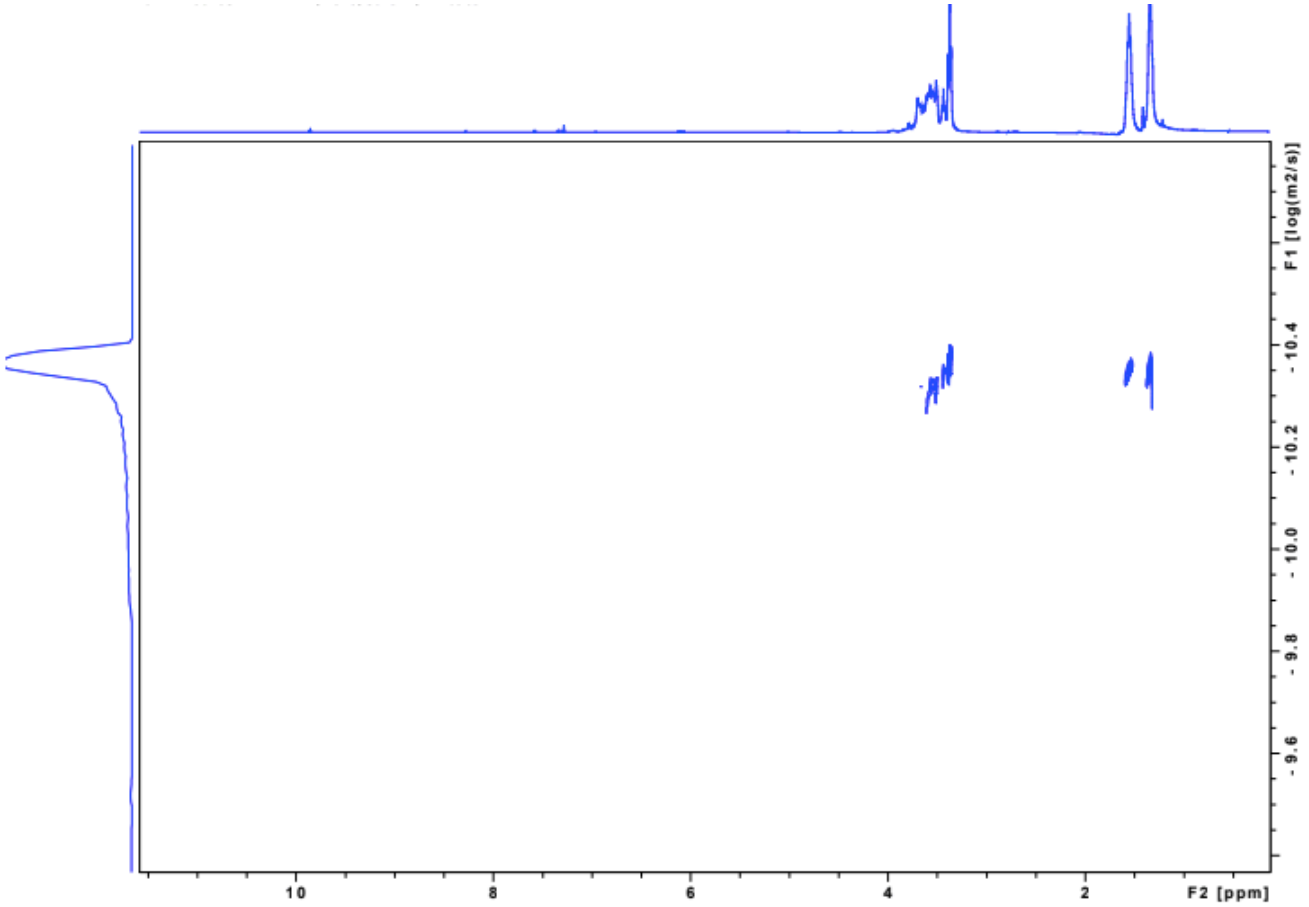

Figure S26. DOSY-NMR of the copolymerization product of oxepane and epichlorohydrin (400 MHz, $CDCl_3$, 25 °C).

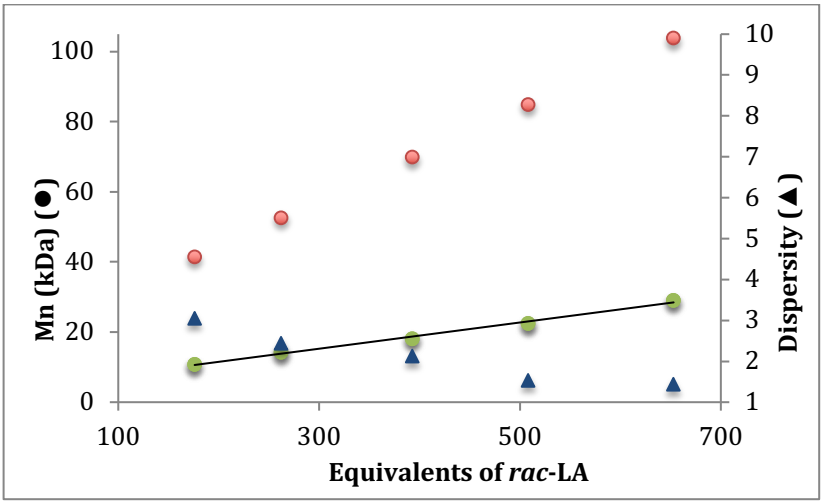

Figure S27. Plot of observed M_n (•) and dispersities (▲) for polymers as a function of equivalents of rac-LA added per equivalent of 3 (130 °C, 1 h). Theoretical molecular weight calculated based on conversions is displayed on top (red circles). Polymerization was carried out in the presence of 100 equivalents of epichlorohydrin and monitored to 90% conversion of rac-LA by ^{1}H NMR spectroscopy.

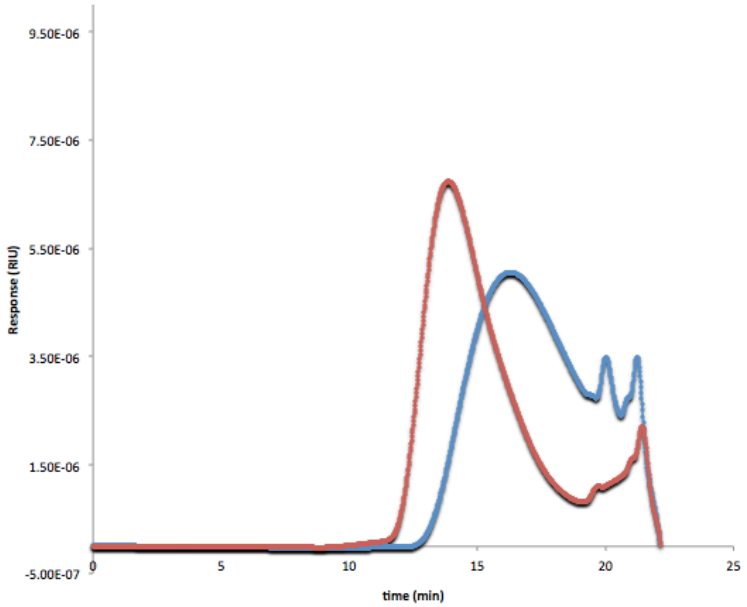

Figure S28. GPC traces of the polymers product of homopolymerization of epichlorohydrin (blue) and copolymerization of epichlorohydrin and THF (red).

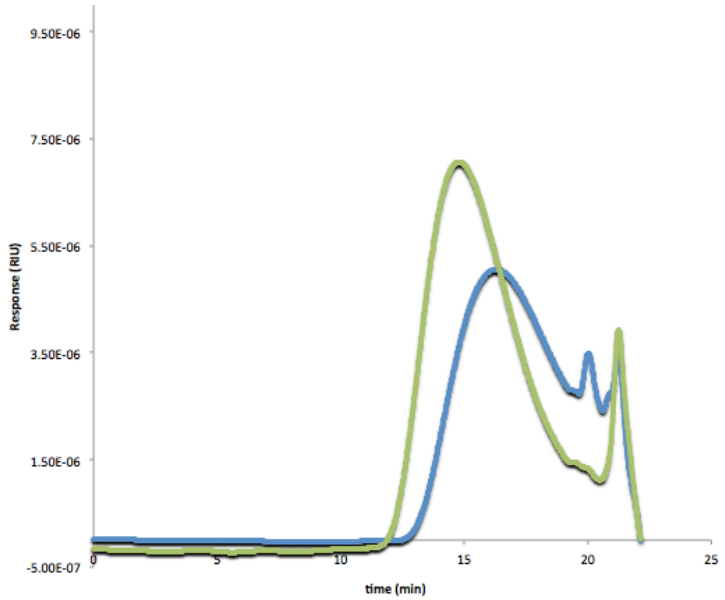

Figure S29. GPC traces of the polymers product of homopolymerization of epichlorohydrin (blue) and copolymerization of epichlorohydrin and oxetane (green).

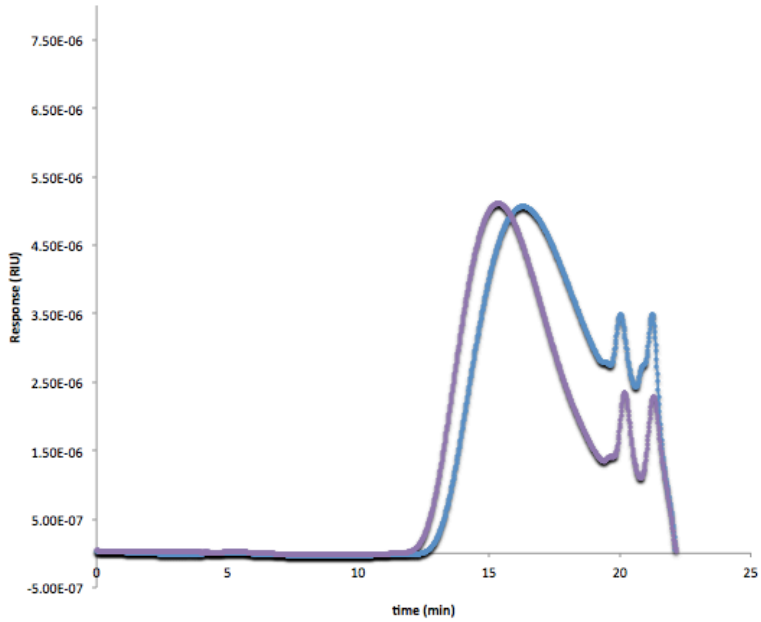

Figure S30. GPC traces of the polymers product of homopolymerization of epichlorohydrin (blue) and copolymerization of epichlorohydrin and oxepane (purple).

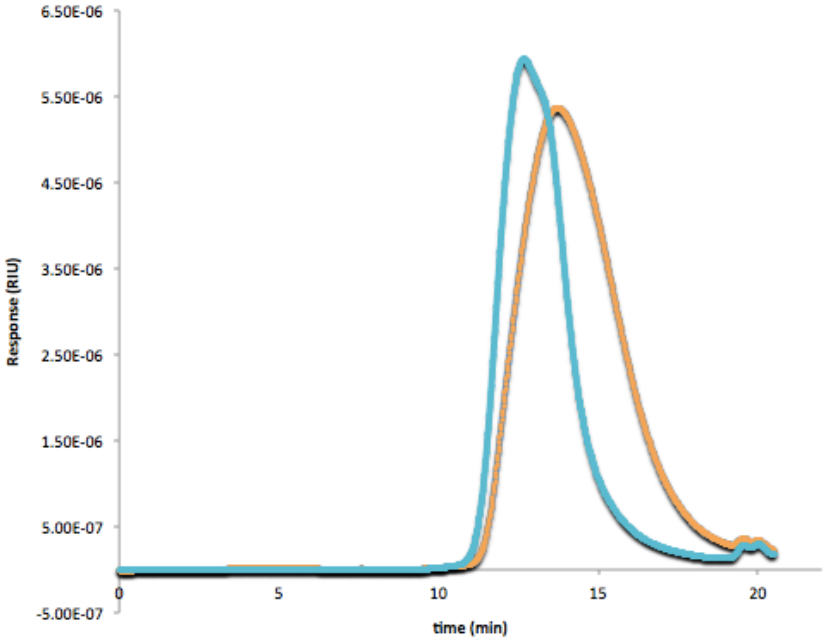

Figure S31. GPC traces of the polymers product of copolymerization of 200 equivalents of epichlorohydrin with 262 equivalents of rac-lactide (orange) copolymerization of 200 equivalents of epichlorohydrin with 653 equivalents of rac-lactide (light blue).

E. Mechanistic Studies

In the truest sense of the word these cationic complexes should not be called *catalysts*, and should be called instead *initiators* for the ROP of epoxides and other cyclic ethers. This since they don't follow a typical coordination-insertion mechanism (*vide infra*) and their structure is irreversibly altered during the polymerization conditions, as evidenced during NMR-monitoring of these reactions (considering a cationic mechanism, the cationic indium center should turn into an indium alkoxide species after initiation). They can, however be called *precatalysts* for lactide polymerization, forming an active species after their reaction with epoxides (putative indium-alkoxide species), which polymerizes lactide in a more controlled coordination-insertion mechanism (*vide infra*).

Evidence strongly supports a cationic mechanism for epoxide polymerization and coordination insertion for lactide polymerization.

1. Polymerization of racemic propylene oxide (PO) with enantiopure cationic complex (R,R)-[(ONNO)In•$(THF)_2$][SbF_6] did not improve at all the regio- or stereo-selectivity compared to the same polymerization using (±)-[(ONNO)In•$(THF)_2$][SbF_6] (as found by ^{13}C NMR). This indicates no influence of the structure around the metal center in the polymer architecture.

2. The counterion effect is in agreement with a cationic mechanism (higher activity for the complex with the more stabilizing counterion). Furthermore, complex formed with a more coordinating triflate anion (OTf), (±)-[(ONNO)In•(THF)][OTf] is incapable of epoxide polymerization.

3. The neutral precursor (±)-(ONNO)InCl of the cationic species is also incapable of epoxide polymerization.

4. MALDI-TOF spectrometry analysis of polymers revealed the presence of cyclic oligomers (no chain-end), which is a consequence of backbiting in cationic mechanisms.

5. Comparison to a more traditional Lewis acid BF_3•(Et_2O), under the conditions studied shows that (±)-[(ONNO)In•$(THF)_2$][SbF_6] (**3**) is more active in the polymerization of epichlorohydrin and produces polymer with high molecular weight (BF_3•(Et_2O) produces only low molecular weight oligomers that could not be precipitated in methanol (Table S3, entries 1-2).

6. In an experiment where epichlorohydrin was ring-opened to high conversions and then rac-lactide was added in-situ complex **3** was active in the ROP of lactide, forming high molecular weight copolymers. BF_3•(Et_2O) was not active in this reaction, yielding no polymer upon precipitation with methanol (Table S3, entries 3-4).

7. Rac-LA cannot be polymerized by (±)-[(ONNO)In•$(THF)_2$][SbF_6] (**3**) either in the melt (130 ºC, 1h) or at room temperature (25 ºC, 72h). In an experiment where rac-LA and epichlorohydrin were added at the same time to (**3**) and monitored at room temperature, it was seen that after 72h of reaction only the epoxide had been converted to polymer (Table S4, entry 2). This is clear indication of a cationic mechanism.

8. In reactions where an equimolar mixture rac-LA and ECH are polymerized at room temperature, rac-LA is not polymerized until the conversion of epoxide reaches a high level, but hinders the ROP rate of ECH significantly. These results indicate that rac-LA is not polymerized by the same cationic mechanism as ECH and most probably it's polymerized by a coordination-insertion mechanism, that only comes into play when the concentration of ECH has reached a low level (Table S3, entry 3).

9. DSC Analysis of the products obtained by the polymerization of ECH and other cyclic ethers (THF, oxetane and oxepane) rule out the possibility of a block copolymerization, as there was only one T_g transition found in those products (See SI). For the ECH/THF copolymer and for the ECH/oxetane copolymer, the T_g values found are between the values for the two respective homopolymers (−22/−86 ºC for PECH/PTHF and −22/−71 ºC for PECH/Polyoxetane), and therefore both copolymers can be considered statistical copolymers.

10. Interestingly, ECH/LA copolymer synthesized in the melt at 130 ºC, also showed only one glass transition temperature, which was intermediate between the values for the two respective homopolymers (−22/+59 ºC). We attribute this to extensive trans-esterification at high temperatures in the copolymer, resembling an statistical copolymer. On the other hand, the copolymer synthesized in two steps at room temperature (Table 1, entry 3) shows a well-defined glass transition for the ECH portion of the polymer and a glass transition for the LA portion, overlapping with the melting curve of ECH portion. This copolymer synthesised at room temperature can be considered a block copolymer.

11. We tested the living character of the ROP of epoxides with compound **3** by sequential addition of epoxide monomer after the polymerization of a first batch at room temperature and did not found an increase in molecular weight by GPC with the second addition. Repeating the same experiment at 80 ºC, resulted in a bimodal distribution after the second addition, one with the same molecular weight before the second addition and the other with higher molecular weight (See section on living polymerization).

Table S3. Copolymerization of epichlorohydrin and rac-lactide at 25 °C.

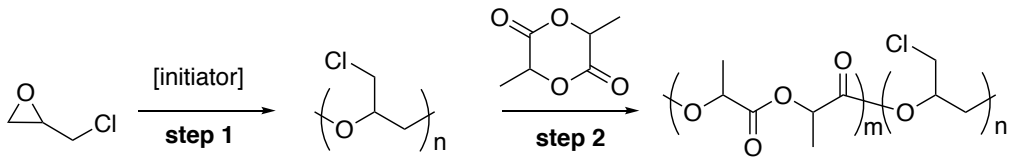

	Initiator	[ECH]/ [initiator]	time (h) step 1	conv. (%)[a] step 1	Mn (10^{-3} Da)[b]	Đ	[LA]/ [initiator]	time (h) step 2	conv. (%)[a] step 2	Mn (10^{-3} Da)[b]	Đ
1	3	200	18	96	**76.5**	**1.13**					
2	BF_3•(Et_2O)		18	72	~2000[c]	-					
3	3		18	96			176	52	52	**97.3**	**1.14**
								96	72	**120.1**	**1.15**
4	BF_3•(Et_2O)		18	72				52	0	-	-

Reactions were performed in dichloromethane at 25 °C. [Initiator] = 32.0 mM, [epoxide] = 6.4 M, [LA] = 5.6 M. [a]Conversion was monitored by ^{1}H NMR spectroscopy. [b]Determined by GPC measurements in THF. [c]Approximated from MALDI-TOF experiment.

Table S4. Copolymerization of epichlorohydrin and rac-lactide at 25 °C.

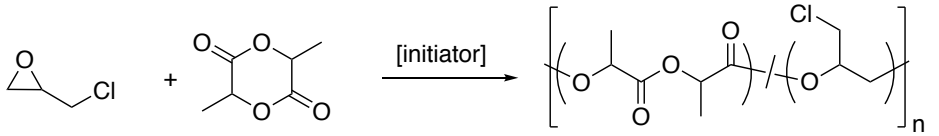

	Initiator	[ECH]/ [initiator]	[LA]/ [initiator]	time (h)	conv. (%)[a] ECH	conv. (%)[a] LA
1	3	0	176	72		0
2	**3**	200	176	18	37	0
				52	62	0
				72	69	0

Reactions were performed in dichloromethane at 25 °C. [Initiator] = 32.0 mM, [epoxide] = 6.4 M, [LA] = 5.6 M. [a]Conversion was monitored by ^{1}H NMR spectroscopy. [b]Determined by GPC measurements in THF.

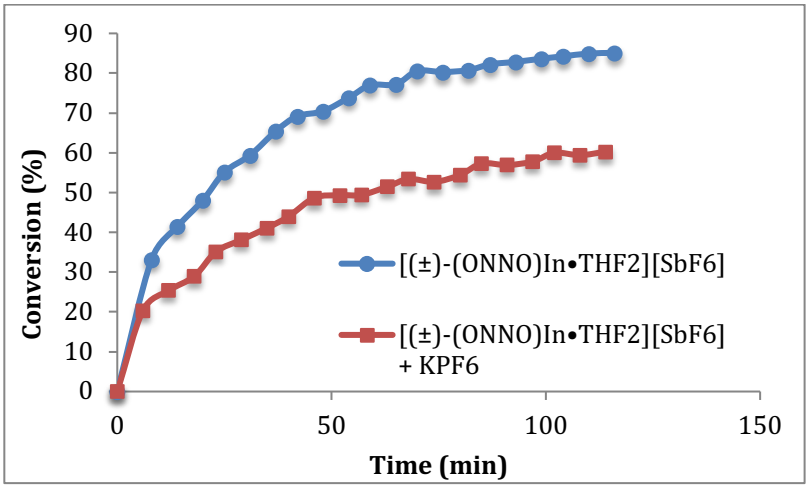

Figure S32. Effect of addition of KPF_6 on the polymerization of 1,2-epoxy-5-hexene by $[(ONNO)In(THF)_2][SbF_6]$ (**3**) at 50 °C. The ROP reaction was monitored by ^1H NMR spectroscopy.

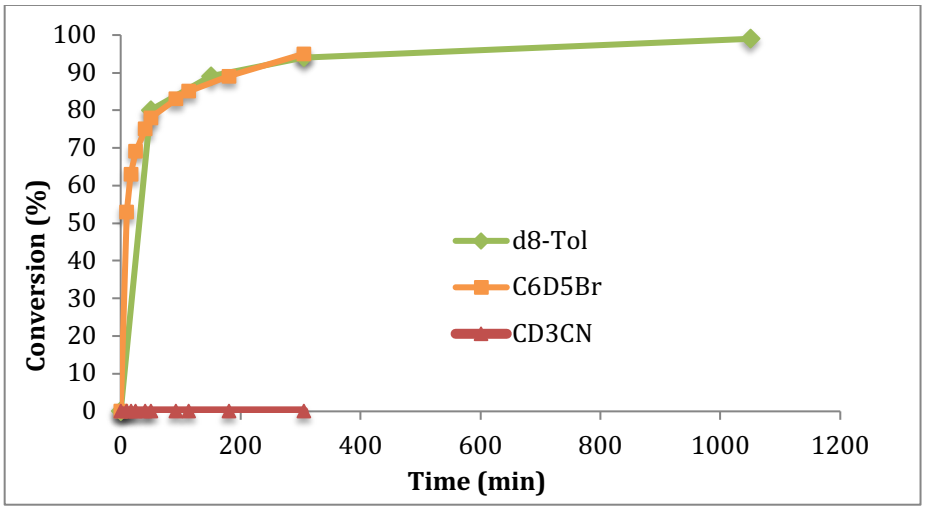

Figure S33. Effect of different solvents in the polymerization of 1,2-epoxy-5-hexene by $[(ONNO)In(THF)_2][SbF_6]$ (**3**) at 25°C. The ROP reaction was monitored by ^1H NMR spectroscopy.

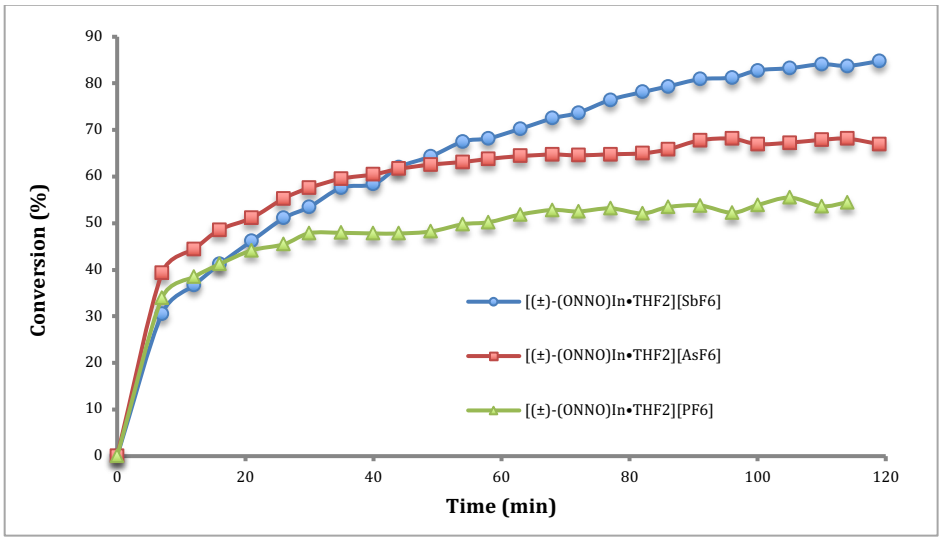

Figure S34. Comparison of activity of different cationic indium species synthesized. Reactions were performed in bromobenzene-d5 at 40 °C for 2 h. [cat] = 28.0 mM, [1,2-epoxy-5-hexene] = 2.8 M. The ROP reaction was monitored by ^{1}H NMR spectroscopy.

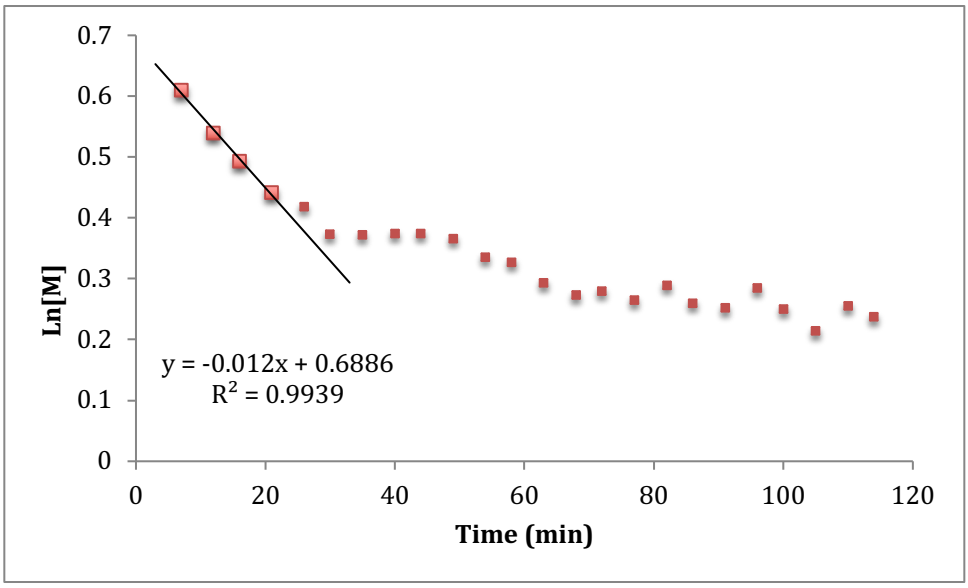

Figure S35. First order kinetic plot for the polymerization of 1,2-epoxy-5-hexene by [(ONNO)In(THF)$_2$][PF$_6$] (**1**) at 40 °C. The ROP reaction was monitored by ^{1}H NMR spectroscopy.

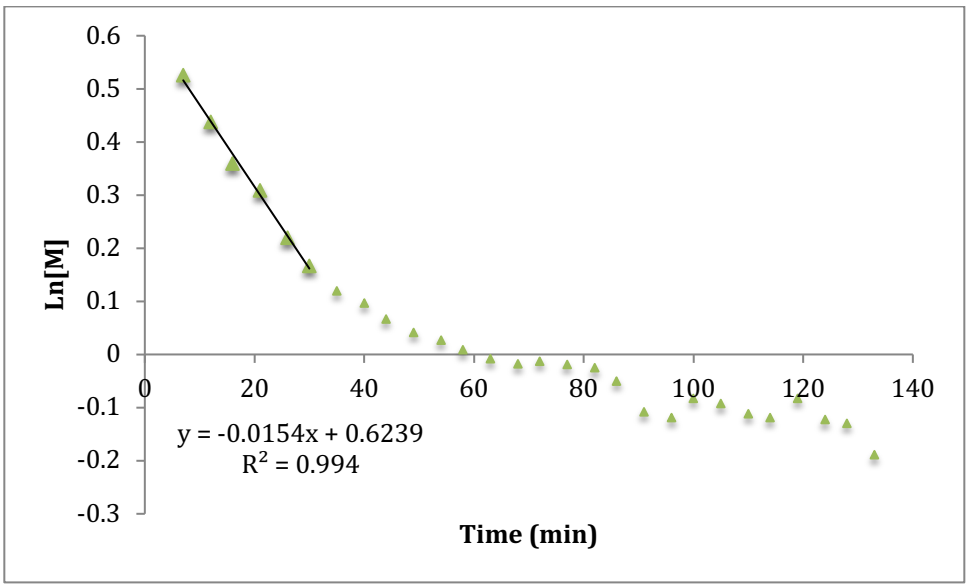

Figure S36. First order kinetic plot for the polymerization of 1,2-epoxy-5-hexene by $[(ONNO)In(THF)_2][AsF_6]$ (**2**) at 40 °C. The ROP reaction was monitored by ^1H NMR spectroscopy.

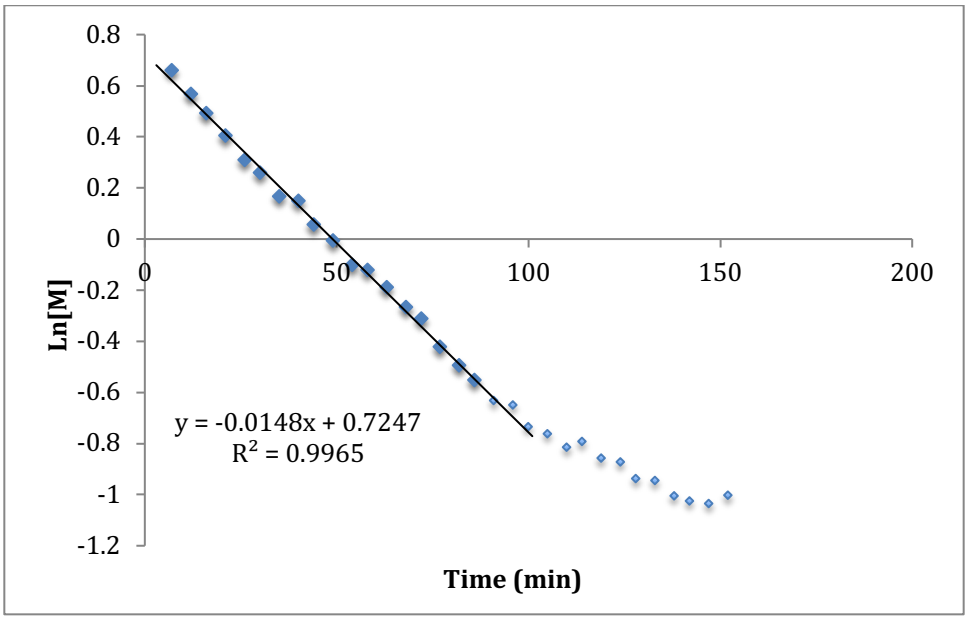

Figure S37. First order kinetic plot for the polymerization of 1,2-epoxy-5-hexene by $[(ONNO)In(THF)_2][SbF_6]$ (**3**) at 40 °C. The ROP reaction was monitored by ^1H NMR spectroscopy.

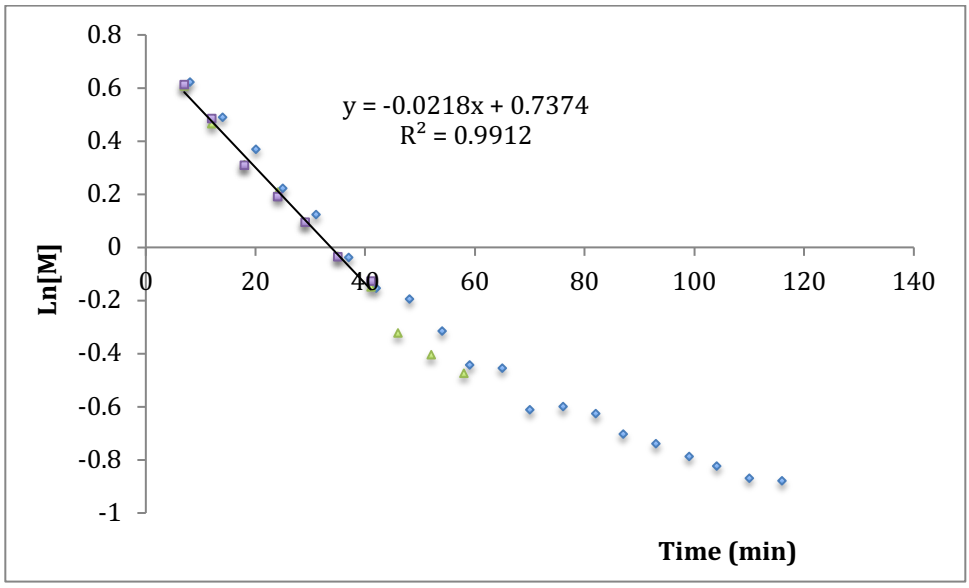

Figure S38. First order kinetic plot (3 different replicates) for the polymerization of 1,2-epoxy-5-hexene by $[(ONNO)In(THF)_2][SbF_6]$ (**3**) at 50 °C. The ROP reaction was monitored by ^1H NMR spectroscopy.

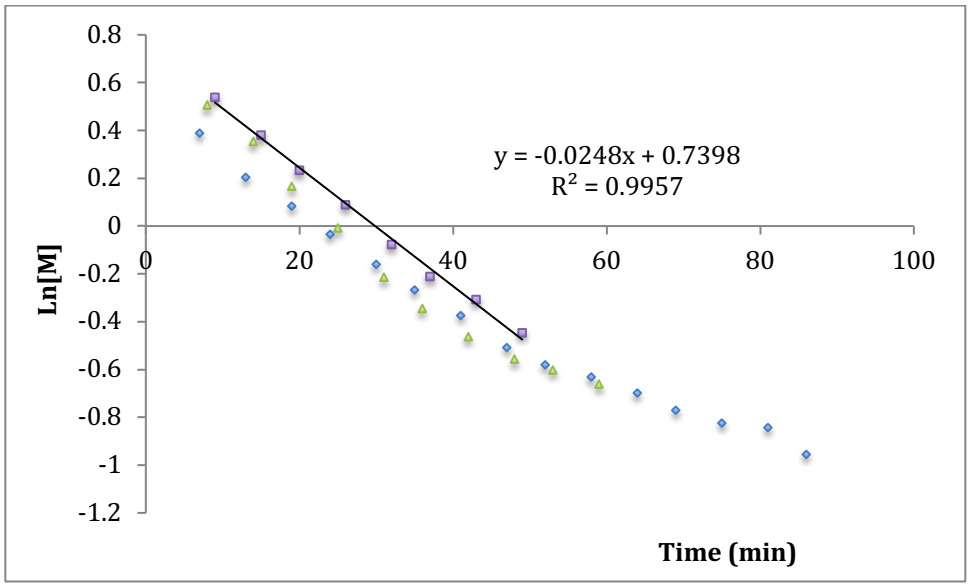

Figure S39. First order kinetic plot (3 different replicates) for the polymerization of 1,2-epoxy-5-hexene by $[(ONNO)In(Me\text{-}THF)_2][SbF_6]$ (**5**) at 50 °C. The ROP reaction was monitored by ^1H NMR spectroscopy.

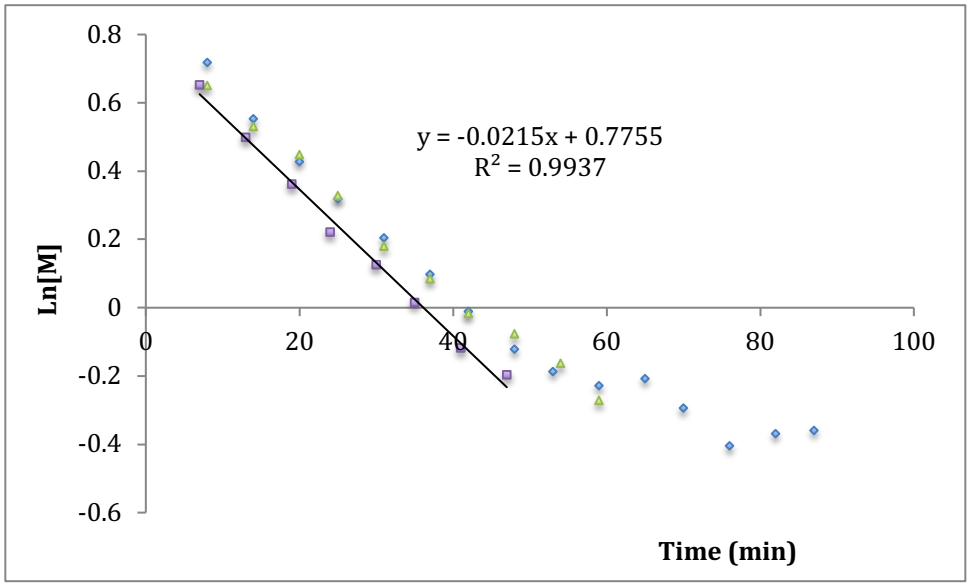

Figure S40. First order kinetic plot (3 different replicates) for the polymerization of 1,2-epoxy-5-hexene by $[(ONNO)In(THP)_2][SbF_6]$ (**6**) at 50 °C. The ROP reaction was monitored by ^1H NMR spectroscopy.

F. Thermal analysis of polymers

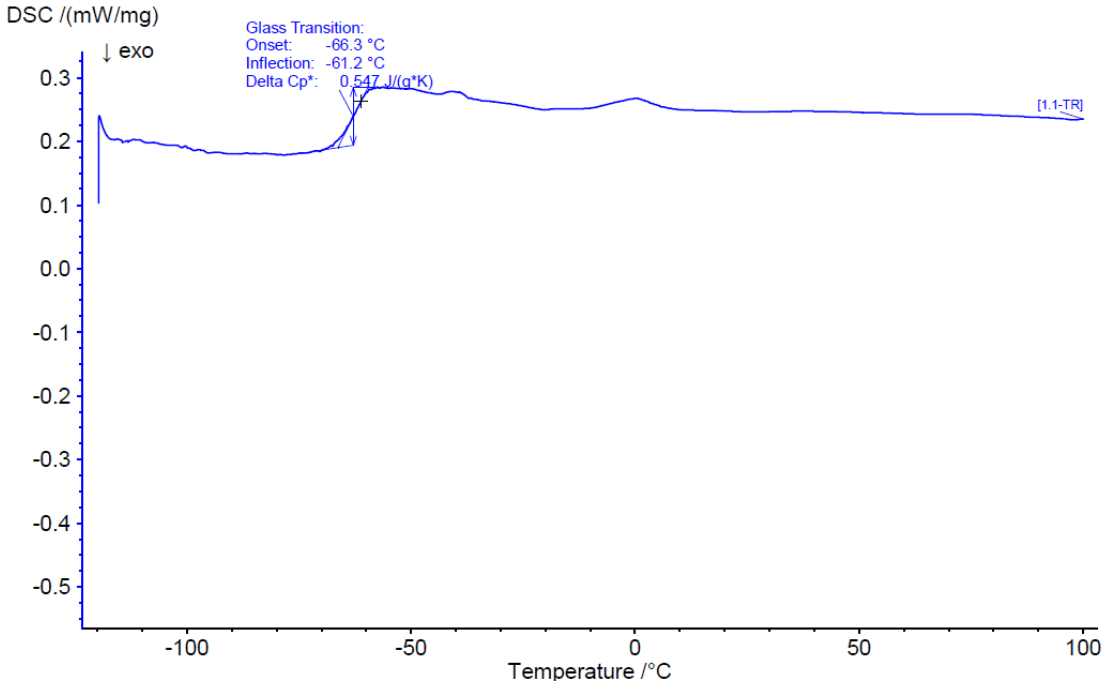

Figure S41. DSC thermogram of the polymer product of copolymerization of epichlorohydrin and THF.

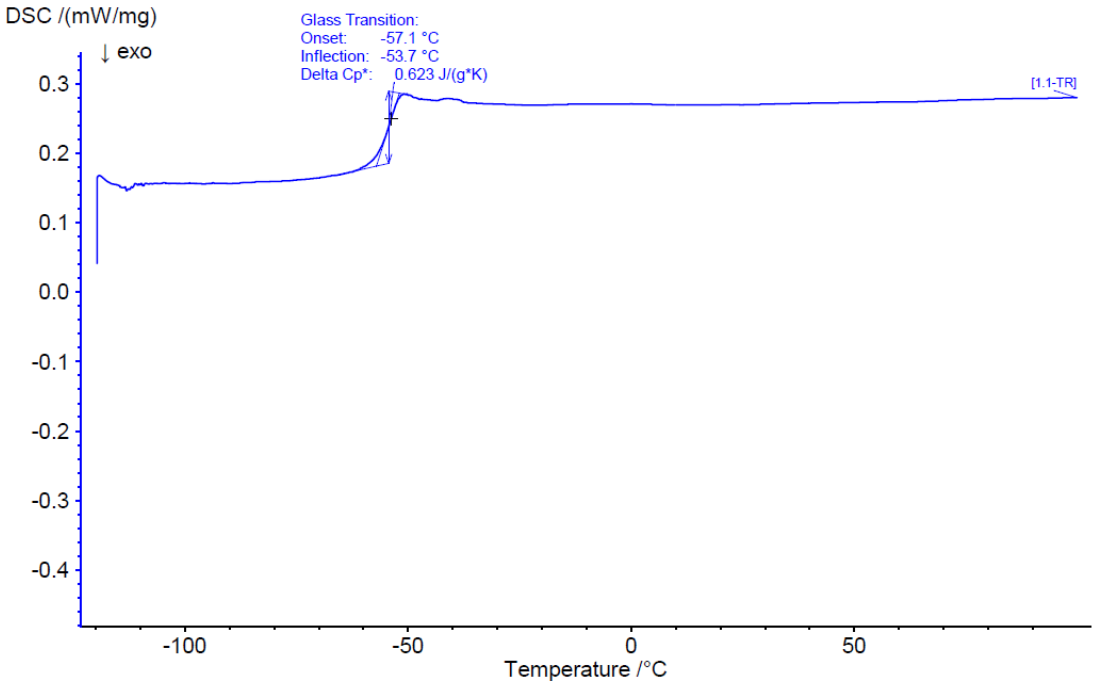

Figure S42. DSC thermogram of the polymer product of copolymerization of epichlorohydrin and oxetane.

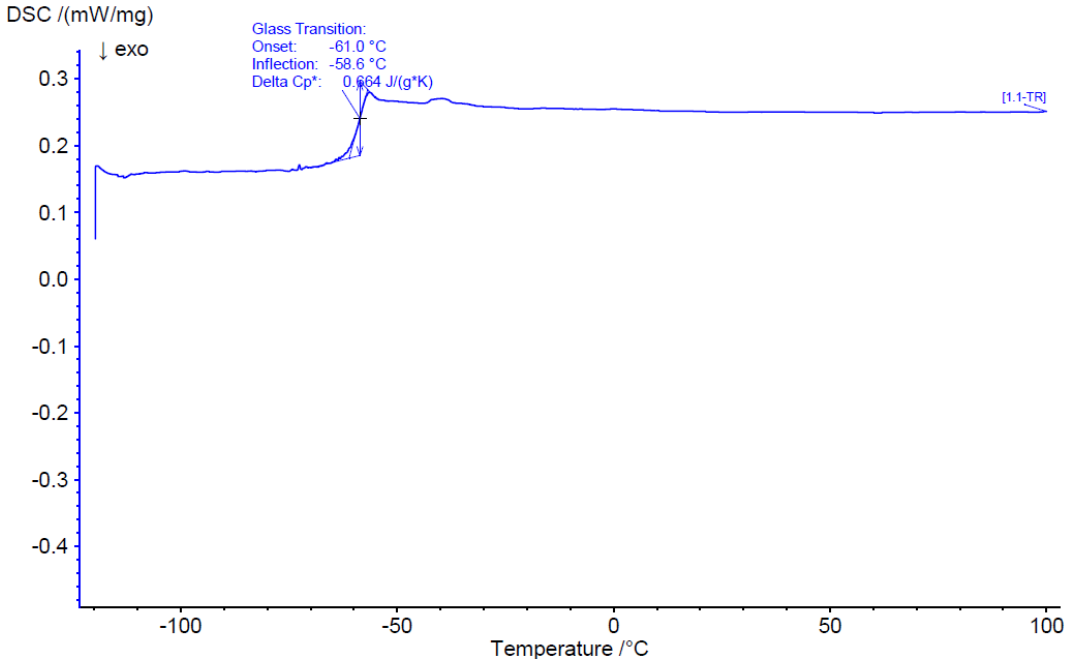

Figure S43. DSC thermogram of the polymer product of copolymerization of epichlorohydrin and oxepane.

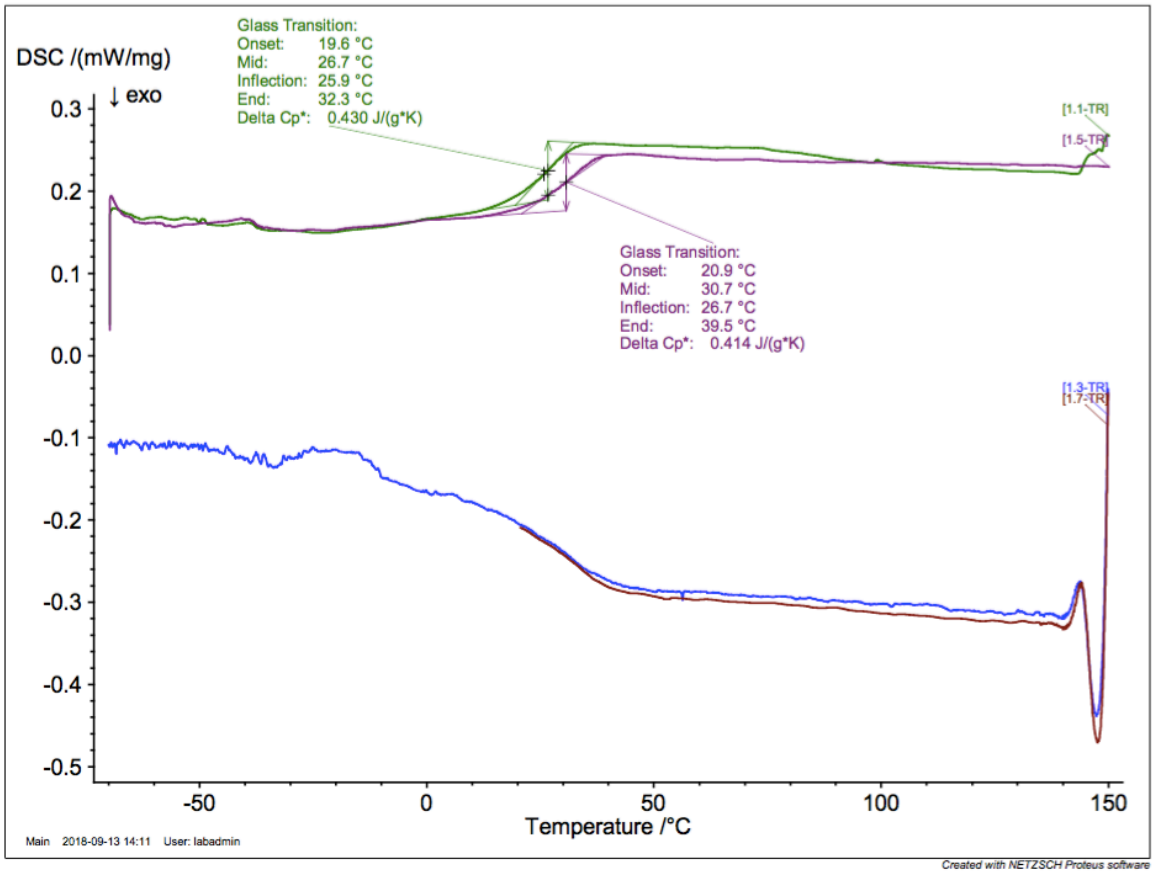

Figure S44. DSC thermogram of the polymer product of copolymerization of epichlorohydrin and lactide at 130 ºC.

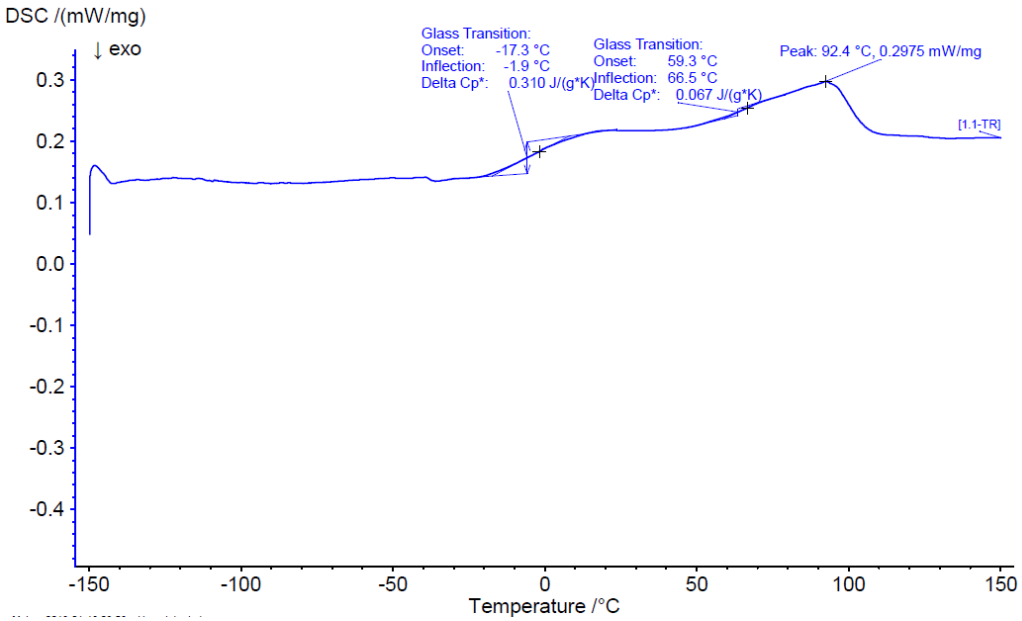

Figure S45. DSC thermogram of the polymer product of block-copolymerization of epichlorohydrin and lactide at 25 ºC.

G. Living experiments

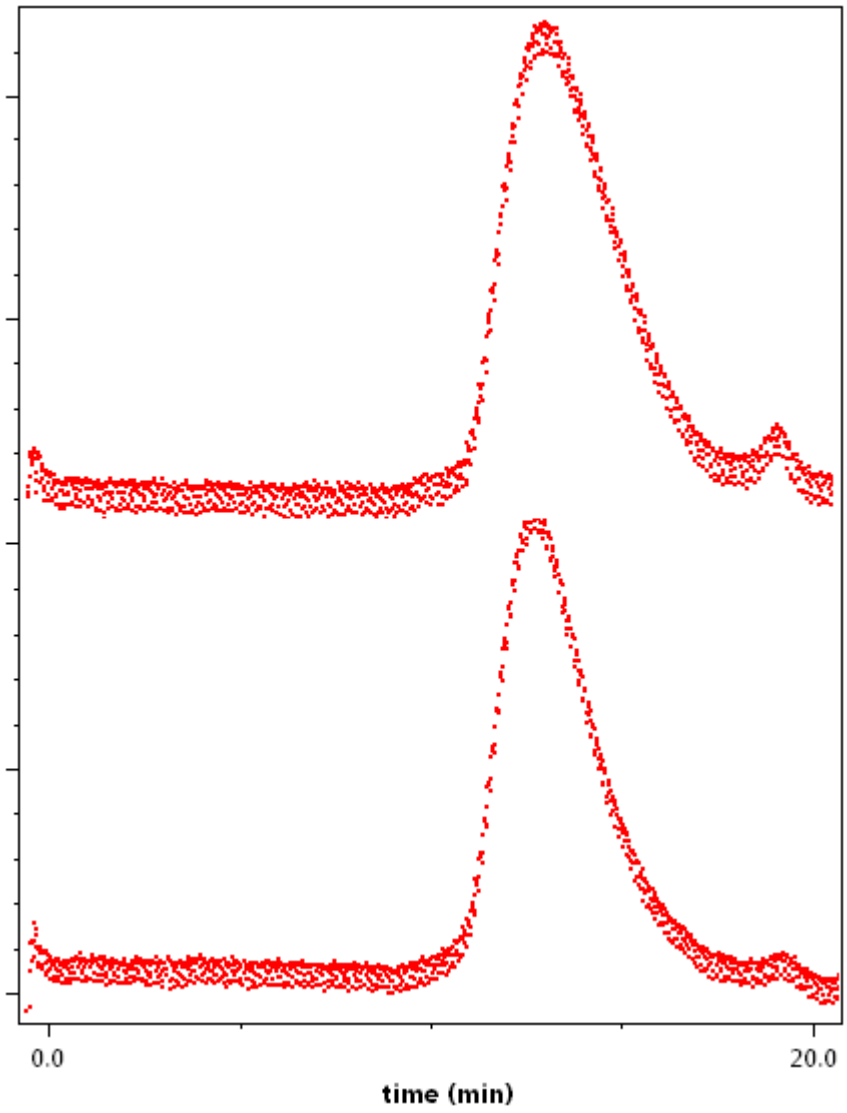

Figure S46. Molecular weight distribution of the product of polymerization of 100 eq. of 1,2-epoxy-5-hexene with (**4**) at 25 °C (bottom). Subsequent addition of another 100 eq. to the same system still produces conversion, but no change in the molecular weight of the product (top).

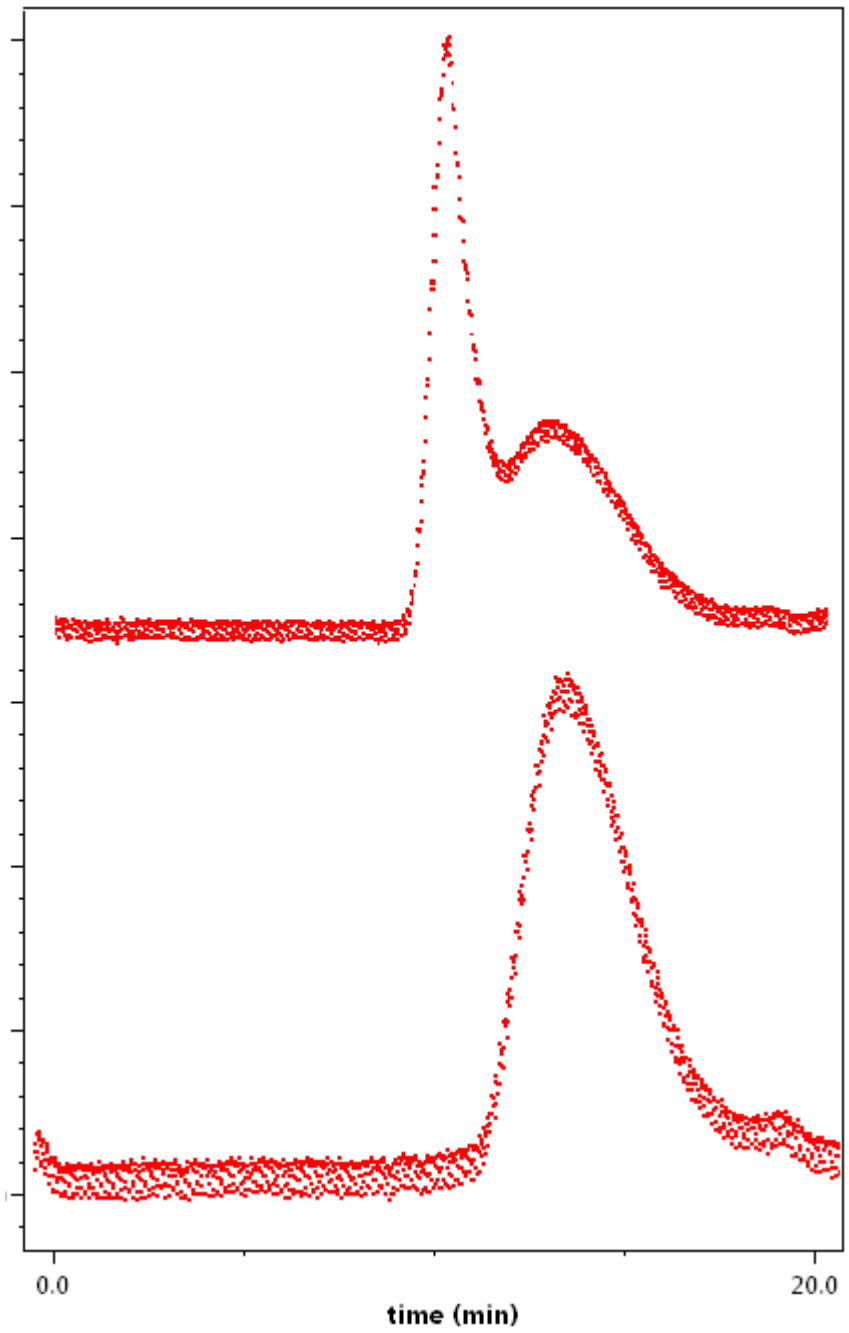

Figure S47. Molecular weight distribution of the product of polymerization of 100 eq. of 1,2-epoxy-5-hexene with (**4**) at 80 °C (bottom). Subsequent addition of another 100 eq. to the same system still produces conversion at 80 °C, yielding a product with a bi-modal distribution of molecular weight (top).

H. References

1. D. C. Aluthge, B. O. Patrick and P. Mehrkhodavandi, *Chem. Commun.*, 2013, **49**, 4295-4297.